Madalena Marques

EVALUATION OF PATIENTS WITH NEUROLOGICAL DISEASES DUE TO NUCLEOTIDE REPEAT EXPANSIONS

UNIVERSIDADE D COIMBRA
1 2 9 0

UNIVERSIDADE D
COIMBRA

Madalena Maria Petronilo Marques

EVALUATION OF PATIENTS WITH NEUROLOGICAL DISEASES DUE TO NUCLEOTIDE REPEAT EXPANSIONS

VOLUME 1

Dissertação no âmbito do Mestrado em Biotecnologia Farmacêutica orientada pela Professora Doutora Maria do Rosário Almeida e supervisionada por Professor Doutor Luís Pereira de Almeida e apresentada à Faculdade de Farmácia da Universidade de Coimbra.

Setembro de 2022

UNIVERSIDADE D
COIMBRA

Madalena Maria Petronilo Marques

EVALUATION OF PATIENTS WITH NEUROLOGICAL DISEASES DUE TO NUCLEOTIDE REPEAT EXPANSIONS

VOLUME 1

Dissertação no âmbito do Mestrado em Biotecnologia Farmacêutica orientada pela Professora Doutora Maria do Rosário Almeida e supervisionada por Professor Doutor Luís Pereira de Almeida e apresentada à Faculdade de Farmácia da Universidade de Coimbra.

Setembro de 2022

FACULDADE DE FARMÁCIA
UNIVERSIDADE D
COIMBRA

Evaluation of Patients With Neurological Diseases Due to Nucleotide Repeat Expansions

Madalena Maria Petronilo Marques

Tese no âmbito do Mestrado em Biotecnologia Farmacêutica, orientada pela Professora Doutora Maria do Rosário Almeida, supervisionada pela Professor Doutor Luís Pereira de Almeida apresentada à Faculdade de Farmácia da Universidade de Coimbra.

Setembro 2022

Agradecimentos

Uma tese de Mestrado é um percurso longo, com muito desafios no qual te obrigam a crescer, sem o qual não seria possível sem o apoio de várias pessoas.

À minha orientadora, Doutora Maria do Rosário Almeida, em primeiro lugar por ter me aceitado neste projeto de investigação. Obrigado por ter paciência, pela confiança que depositou em mim.

Ao meu orientador ligado à Faculdade de Farmácia da Universidade de Coimbra, Doutor Luís Pereira de Almeida, por aceite o convite e supervisionado esse percurso.

Ao Doutor Miguel do Laboratório de Citogenética, sem a qual não seria possível concretizar um dos objetivos desta tese.

À Doutora Ana Santos, por diretamente ou indiretamente ter acompanhado este projeto, obrigado pelo companheirismo e disponibilidade para tirar dúvidas.

Aos clínicos do serviço de neurologia do Hospital Universitário de Coimbra, por disponibilizarem os dados clínicos e demográficos dos doentes necessários para realização da tese.

Por fim quero agradecer, à minha família, por ter apoiado neste percurso tão importante. Especialmente ao meu irmão, por ter ajudado na escrita da tese.

A todas aqueles que diretamente ou indiretamente me ajudaram e apoiaram em todo neste percurso.

Index

List of figures

List of tables

List of abbreviations

Units:

ºC- Celsius Degrees

uL- Microliter

mL- Milliter

uM- Micromolar

mM- Milimolar

nm- Nanometer

g- Gram

ng- Nanogram

min- Minutes

KDa-kilodalton

sec- Seconds

U- Enzyme Unit

bp- Basis Pairs

rxn- reaction

A-Z:

3' UTR- 3' untranslated region

5' UTR- 5' untranslated region

AF- Atrial fibrillation

ALS- Amyotrophic lateral sclerosis

ATXN3- *Ataxin-3*

bvFTD- behavioral variant Frontotemporal Dementia

C9orf72- *Chromosome 9 Open Reading Frame 72*

CE- Capillary Electrophoresis

CNS- Central Nervous System

ddNTPs- Dideoxynucleotide triphosphates

DNA- Deoxyribonucleic acid

DPRs- dipeptide protein repeats

dNTPs- Deoxynucleotide triphosphates

ddNTPs- Dideoxynucleotide triphosphates

ECG-Electrocardiogram

EXO- exonuclease I

FTLD- Frontotemporal Lobar Degeneration

FUS- FUS RNA binding protein

FRDA- Friedreich Ataxia

FXN- *Frataxin*

gDNA- Genomic Deoxyribonucleic acid

GRN*- Granulin*

HTT- *Huntingtin*

HD- Huntington Disease

HRE- Hexanucleotide Repeat Expansion

JHD- Juvenile Huntington Disease

MAPT- Microtubule Associated Protein Tau

MJD- Machado Joseph Disease

mHTT- mutant huntingtin

NTC- No Template Control

PCR- Polymerase chain reaction

polyQ- Polyglutamine

RNA- Ribonucleic acid

RBP- RNA binding proteins

RP-PCR- Repeat Primed polymerase chain reaction

SAP- shrimp alkaline phosphatase

SCA3- Spinocerebellar ataxia type 3

SCAs- Spinocerebellar Ataxia

SOD1- Superoxide dismutase type 1

TARDBP- TAR DNA Binding Protein

TBE- Tris borate ethylenediaminetetraacetic acid

TBK1- TANK-binding kinase 1

TDP-43- TAR DNA binding protein 43

TNF- Tumor Necrosis Factor

TP-PCR- Triplet primed repeat polymerase chain reaction

Abstract

Repeat expansion disorders are a class of genetic diseases that are caused by expansions in DNA repeats. These repeats can be of various sizes such as: trinucleotide, tetranucleotide, hexanucleotide or longer. The affected patients have specific phenotypes and onset age and these diseases are often associated with the phenomenon of anticipation. Thus, the signs and symptoms tend to become more severe and/or appear at an earlier age as the disorder is passed from one generation to the next. At the moment, there are over 40 distinct diseases caused by DNA repeat expansions. In the present work, we focus our study on the genetic characterization of patients with repeat expansion disorders, such as: Friedreich's Ataxia, Frontotemporal Lobar Degeneration, Amyotrophic Lateral Sclerosis, Huntington's Disease and Machado Joseph Disease. We aimed to set up different molecular techniques to detect and quantify the size of the pathological expansions in these patients.

The Friedreich's ataxia (OMIM # 229300) is an autosomal recessive spinocerebellar ataxia. More than 95% of patients have expanded GAA trinucleotide repeats in intron 1 of the *FXN* gene whereas the remaining 5% of the cases have point mutations in this gene. Therefore, the mutation analysis in the *FXN* gene was optimized as well as the analysis of the GAA repeat expansions in this gene and ten patients followed in the Neurology Department of CHUC have been studied. None of the patients harbor any point mutation or pathogenic repeat expansions in *FXN* gene. Thus, we could not confirm the Friedreich's Ataxia diagnosis in any of the patients referred with the suspected clinical diagnosis of Friedreich Ataxia.

The Frontotemporal Lobar Degeneration (OMIM # 600274) and the Amyotrophic Lateral Sclerosis (OMIM # 105550) are neurodegenerative disorders with an onset age typically lower than 55 years. They are autosomal dominant diseases in which an hexanucleotide repeat expansion in the C_9orf_{72} gene is the most common genetic cause. Therefore, in the present study, a new method was set up to quantify the size of the expanded allele in fifty-six patients known as carriers of the pathogenic G_4C_2 expansion. Thus, 53 individuals were identified with one expanded allele (>145 G_4C_2 repeats), while 3 patients harbor a smaller expanded allele (ranging from 38-78 G_4C_2 repeats).

The Huntington's Disease (OMIM #143100) is a progressive brain autosomal dominant disease, caused by an expansion of a CAG trinucleotide repeat encoding in exon 1 of the *HTT* gene. Thus, ten patients were evaluated by a new method set up in the laboratory to detect the presence of an expanded allele in the *HTT* gene and in five patients it was possible to confirm the clinical diagnosis of Huntington's Disease.

The Machado Joseph Disease (OMIM # 109150) is an autosomal dominant neurodegenerative disease of late onset that predominantly involves the cerebellar, pyramidal, extrapyramidal, motor neuron, and oculomotor systems. The genetic cause is an unstable CAG repeat expansion mutation in the coding region of the *ATXN3* gene.

Thus, we developed an in-house method, involving STR-PCR and RP-PCR assays, to detect the number of CAG repeats expansions in the *ATXN3* gene in sixteen patients. Of those, four were identified as having an expanded allele typical of Machado Joseph Disease.

Therefore, in the present study we were able to set up several molecular approaches to detect the pathological expansions in patients with different Neurological diseases such as: Friedreich's Ataxia, Frontotemporal Lobar Degeneration, Amyotrophic Lateral Sclerosis, Huntington's Disease and Machado Joseph Disease, using commercial kits and/or in-house methods. In the future these methods will be included in the Neurogenetic laboratory in a routine basis to evaluate patients with the suspected clinical diagnosis of one of these diseases. For those patients to whom we confirmed that they harbor a pathogenic expansion, it is particular important the genetic counselling consultation due to the anticipation phenomenon observed in some of these diseases. Finally, in the future it will be also important to increase the number of patients studied to establish genotype-phenotype correlations.

Key-Words: *FXN*, *ATXN3*, C_9orf_{72}, *HTT,* expansions

Resumo

As doenças causadas por expansões são uma classe de doenças genéticas que resultam da expansão de repetições no DNA. Estas repetições têm vários tamanhos, desde nucleótidos simples, trinucleotideos, tetranucleotideos, hexanucleotideos ou mais longos. Os doentes têm fenótipos específicos e idade de início e estas doenças estão frequentemente associadas ao fenómeno da antecipação. Assim, os sinais e sintomas destas doenças genéticas particulares, tendem a tornar-se mais graves e/ou a aparecer numa idade mais precoce à medida que a doença é transmitida de uma geração para a seguinte. Até ao momento, existem mais de 40 doenças distintas causadas por repetições de expansões na sequência de DNA. Neste trabalho, centrámos o nosso estudo na caracterização genética de doentes com doenças causadas por repetições de expansões, como por exemplo: Ataxia de Friedreich, Degenerescência Lobar Frontotemporal, Esclerose Lateral Amiotrófica, Doença de Huntington e Doença de Machado Joseph. O nosso objetivo foi estabelecer diferentes técnicas moleculares para detetar e quantificar a dimensão das expansões patológicas nos doentes estudados.

A Ataxia de Friedreich (OMIM # 229300) é uma ataxia espinocerebelar autossómica recessiva. Mais de 95% dos doentes têm a expansão da repetição trinucleotidica GAA no intrão 1 do gene *FXN* enquanto que os restantes 5 % têm uma mutação pontual neste gene. Neste sentido, a análise molecular no gene *FXN* foi otimizada, bem como a deteção das expansões de repetição de GAA neste gene. Foram estudados dez doentes, seguidos no Serviço de Neurologia do CHUC. Em nenhum dos doentes foi identificada qualquer mutação pontual ou expansões de repetições patogénicas no gene *FXN*. Assim, não foi possível confirmar o diagnóstico de Ataxia de Friedreich nos doentes referenciados com suspeitas do diagnóstico clínico de Ataxia de Friedreich.

A Degenerescência Lobar Frontotemporal (OMIM # 600274) e a Esclerose Lateral Amiotrófica (OMIM # 105550) são doenças neurodegenerativas autossómicas dominantes com uma idade de início habitualmente inferior a 55 anos, nas quais uma expansão de repetição hexanucleotídica no gene C_9orf_{72} é a causa genética mais comum. Assim, neste estudo, foi implementado um novo método para quantificar o tamanho do alelo expandido em cinquenta e seis doentes identificados como portadores da expansão patogénica G_4C_2. Assim, foram identificados 53 doentes com um alelo expandido (>145 repetições de G_4C_2), enquanto que em 3 doentes o alelo expandido identificado foi mais pequeno (variando entre 38-78 repetições de G_4C_2).

A doença de Huntington (OMIM #143100) é uma doença neurodegenerativa progressiva autossómica dominante no cérebro, causada por uma expansão de repetição trinucleotidica de CAG no exão 1 do gene *HTT*. Assim, dez doentes foram avaliados por um novo método implementado no Laboratório de Neurogenética para detetar a presença de um alelo expandido no gene *HTT*, e em cinco doentes foi possível confirmar o diagnóstico clínico de Doença de Huntington.

A doença de Machado Joseph (OMIM # 109150) é uma doença neurodegenerativa autossómica dominante de início tardio que envolve predominante os sistemas cerebelares, piramidal, extrapiramidal, neurónio motor, e oculomotor. A causa genética é uma mutação instável que envolve a expansão da repetição de CAG na região codificante do gene *ATXN3*.

Assim, desenvolvemos um método *in-house*, envolvendo STR-PCR e RP-PCR, para detetar o número de expansões de repetições de CAG no gene *ATXN3* em dezasseis doentes, dos quais quatro foram identificados como tendo um alelo expandido típico da doença de Machado Joseph.

Assim, neste estudo tivemos oportunidade de implementar várias técnicas moleculares para detetar as expansões de repetições patogénicas em doentes com diferentes doenças neurológicas, tais como: Ataxia de Friedreich, Degenerescência Lobar Frontotemporal, Esclerose Lateral Amiotrófica, Doença de Huntington e Doença de Machado Joseph, utilizando kits comerciais e/ou métodos *in-house*. É importante referir que no futuro, estes métodos serão incluídos no Laboratório de Neurogenética para avaliar doentes com suspeitas clínicas de uma destas doenças. Nos doentes em que confirmámos a presença de uma expansão de repetições patogénicas, é particularmente importante a sua referência bem como a dos seus familiares para uma consulta de aconselhamento genético devido ao fenómeno de antecipação observado em algumas destas doenças. Finalmente, no futuro será importante aumentar o número de doentes estudados com cada umas destas patologias no sentido estabelecer correlações genótipo-fenótipo.

Palavra Chave: *FXN*, *ATXN3*, *C_9orf_{72}*, *HTT*, expansão

1.Introduction

1.1. Genetic Diseases

Genetic diseases are caused in whole or in part by a change in the genetic material of the individual. These diseases can be caused by a mutation in one gene (monogenic or Mendelian disorder), by mutations in multiple genes (multifactorial inheritance disorder), by a combination of gene mutations and environmental factors, by mutations in mitochondrial DNA (mitochondrial inheritance) or by changes in chromosomes (changes in the number or structure of chromosomes). There are thousands of known single gene disorders. For example, cystic fibrosis, sickle cell anemia, fragile X syndrome and Huntington's disease. These disorders have different patterns of inheritance, including autosomal dominant inheritance, in which only one copy of a defective gene (from one parent) is needed to cause the condition; autosomal recessive inheritance, in which two copies of a defective gene (one from each parent) are needed to cause the condition; and X-linked inheritance, in which the defective gene is present in the X chromosome. This mode of inheritance can be dominant or recessive.

Within monogenic diseases they can be originated by point mutation, minsense, no-sense, deletion or insertion of a nucleotide, affecting the nucleotide sequence. The minsense mutations, generate a new codon that specifies a different amino acid, leaving the protein with a different amino acid sequence; there are also the non-sense mutations, which convert the specific codon of an amino acid into a stop codon, which produces a smaller protein by interrupting mRNA translation. In general, these types of mutations alter the protein function. And finally, there are frameshit causing a change in the reading frame. This means that all codons downstream (at 3') of the mutation will have a different reading frame from that of the unmutated gene. This results in a significant change in the structure of the encoded protein, since part of the polypeptide encoded by the mutated gene will have a different amino acid sequence than the polypeptide encoded by the normal gene. (SCHWANKER *et al,* 2015)

Moreover, rare diseases are diseases which affect a small number of people compared to the general population. In Europe, when it only affects 1 person in 2000, it is considered rare. However, a disease can be rare in one region, but common in another. For example, thalassemia, an anemia of genetic origin, is rare in northern Europe but common in the Mediterranean region. There are also many common diseases whose variants are rare. While nearly all genetic diseases are rare diseases, not all rare diseases are genetic diseases. There are also very rare forms of infectious diseases, such as auto-immune diseases and rare cancers.

Many rare diseases still have unidentified causes. For many rare diseases, signs can be seen at birth, in childhood, or in adulthood.(ORPHANET, 2016)

1.1.1. Repeat Expansions Disorders

Repeat expansion disorders are a class of genetic diseases that are caused by expansions in DNA repeats. The DNA repeats come in various sizes from single nucleotides to dodecamers or longer. The threshold at which the repeat expansions become symptomatic varies with the specific disease. There are over 40 distinct diseases now known to be caused by these expansions in DNA sequence. Remarkable progress during the last three decades has defined causative mutations that drive pathogenesis in a large number of these diseases. Expansion of CAG, GCG, CTG, CGG, and CAAA repeats both in coding and non-coding sequences in distinct genes results in a diverse group of diseases with mechanisms linked to protein levels or toxicity, RNA, and/or both (Ellerby, 2019). Depending on whether the repetitive sequences are found in the coding area or in the non-coding section of the genome, these disorders are divided into two categories. In the first group, expanded CAGs produce proteins containing an expanded polyglutamine (polyQ) tract, triggering neurodegeneration through toxic gain-of-function mechanisms in Huntington's disease (HD) and Machado Joseph (SCA_3), which are collectively called polyQ diseases. In the second group, the repeat sequences are located in the non-coding region such as 5′-UTR, 3′-UTR, or intron in the genome such as; Friedreich's Ataxia and Amyotrophic Lateral Sclerosis and Frontotemporal Lobar Degeneration linked to C_9orf_{72} (Ueyama e Nagai, 2018). The figure 1 shows the location of the expansions occurs in exonic and intronic regions of the gene.

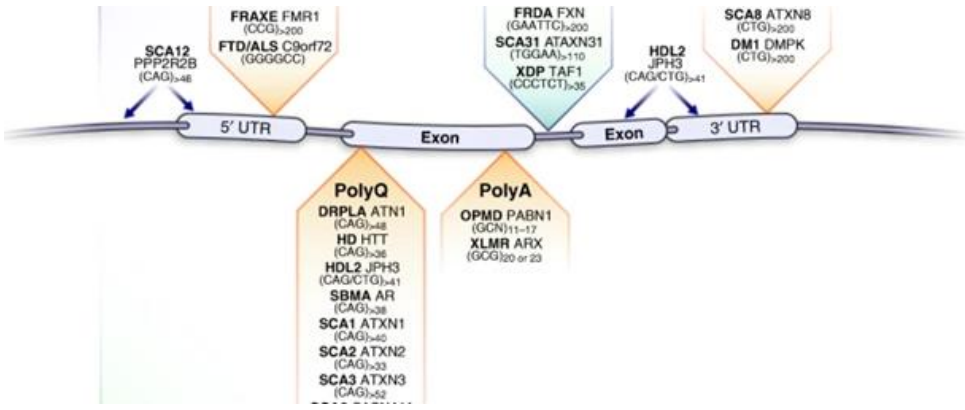

Figure 1- Location of the expansion of DNA repeats (Ellerby, 2019)

1.2. Friedreich Ataxia (FRDA) (OMIM # 229300)

Friedreich's ataxia is an autosomal recessive spinocerebellar ataxia. It is the most common inherited ataxia in Europe, with prevalence differing between regions; between 1 in 20 000 in south-west Europe and 1 in 250 000 in the north and east of Europe. More than 95% of patients have expanded GAA trinucleotide repeats in intron 1. Hence, the disease is characterized by decreased expression of the frataxin (FXN) protein from the *FXN* gene on chromosome 9. The repeat expansion length correlates with age at onset disease severity, and rate of disease progression. The remaining 5% of the cases had a point mutation or a minor deletion allele together with GAA repeats expansion the other allele (Clark *et al.*, 2019). Frataxin is produced from the most abundant *FXN* transcript derived from exons 1–5a. (Delatycki e Bidichandani, 2019)

Both during meiosis and mitosis, the GAA expansion is unstable. Its presence causes an inadequacy, decreased amounts of the *FXN* complete transcript, and suppression of the *FXN* gene expression. The repeat can increase or decrease in size when passed from mother to child but generally decreases in size when passed from father to off- spring (Delatycki *et al.*, 1998). The central nervous system's GAA size analysis revealed signs of mitotic repeat instability. It has been demonstrated that the heart and pancreas are more susceptible to somatic instability than the central nervous system (Delatycki e Bidichandani, 2019). It has been demonstrated that post-zygotic instability rises with age in FRDA patients. FRDA typically manifests as progressively progressing instability, dysmetria, and dysarthria around puberty, which results in the loss of autonomous gait and severe impairments. (Indelicato *et al.*, 2020)

1.2.1. Clinical Features

The Friedreich's Ataxia is a multisystemic disorder, affecting both the central and peripheral nervous systems, the musculo skeletal system, the myocardium and the endocrine pancreas. The first signs of the condition typically appear between the ages of 10 and 16. The combination of cerebellar disease, spinocerebellar tract degeneration, and peripheral sensory neuropathy leads to mixed ataxia. Early onset of gait ataxia results in unstable, although not obviously broad-based, gait. Progressive levels of assistance are required for balance loss and trunk ataxia, with the majority of patients being wheelchair-bound by their 30s. The Limb ataxia affects dexterity and coordination such that basic daily activities become increasingly difficult. Also, nose finger ataxia, upper limb dysdiadochokinesia and impaired heel-shin slide are all common early signs. In addition, dysarthria that consists of slow, slurred speech progresses from early in the disease towards unintelligibility in the advanced stages. The later

stages of disease are associated with pyramidal weakness, particularly of the lower limbs, and distal wasting, which further exacerbates disability. Spasticity has typically been described in the more advanced stages of the disease, contractures and painful muscles spasms can develop secondary to spasticity. Dysphagia is also common and progresses with the disease, and in advanced cases patients require modified diets, and eventually nasogastric feeding or gastrostomy. Common oculomotor abnormalities, include fixation instability with frequent square-wave jerks, and gaze-evoked nystagmus is less common. Aberrant central auditory processing, detectable as abnormal evoked potentials, is common in FRDA, and the associated temporal distortion of stimuli can exacerbate verbal communication difficulties. Bowel symptoms, in the form of constipation or incontinence, are common, and are likely related to reduced mobility and corticospinal pathology. This disease is strongly associated with a cardiomyopathy, and it is thought that cardiac wall abnormalities are present in the majority of patients, though often these will be asymptomatic. The advanced stages of disease are associated with supraventricular tachyarrhythmias, most commonly atrial fibrillation (AF) which, if sustained, can manifest as palpitations. The non-neurological features including scoliosis, pes cavus, cardiomyopathy and diabetes are less frequent amongst the delayed-onset cases. As such, morbidity and mortality are less commonly attribute able to cardiac complications, although of note the ECG is typically abnormal in most cases. The most common cause of death in FRDA is cardiac dysfunction, namely congestive heart failure or arrhythmia. Other causes of death include stroke, ischemic heart disease, and pneumonia. (Cook e Giunti, 2017)

1.2.2. Genetics

As was already established, the majority of FRDA cases are connected to a pathological expansion in the *FXN* gene's first intron, this gene encoded a protein called frataxin, with 130 amino acids and is 14 kDa in size, the figure 2 show a fraxatin protein structure (Cook e Giunti, 2017). The heart, spinal cord, liver, pancreas, and muscles used for voluntary movement are where this protein is found. Frataxin is a protein that is present in cells mitochondria. Frataxin appears to aid in the assembly of clusters of iron and sulfur molecules that are essential to the operation of numerous proteins, including those required for energy production, despite the fact that its exact role is yet unknown (Castaldo *et al.*, 2008)

The frataxin protein is pathologically repressed as a result of the GAA intronic expansion's silencing of the *FXN* gene. There has been substantial research into the processes driving this silencing effect. Position effect variegation, in which GAA repeats cause aberrant

heterochromatization of neighboring genes and leave them transcriptionally inactive in specific cell populations, may be the cause of this gene's silencing. When the transcriptional balance of euchromatic (active transcription) and heterochromatic (inactive transcription) components is balanced, this effect is predicted to occur. This balance is anticipated to shift toward heterochromatin and gene silence in FRDA through open epigenetic processes like DNA methylation and histone modification. Quantitative investigations in peripheral blood mononuclear cells from FRDA patients demonstrated unusually widespread DNA methylation upstream of the repeat expansion at the silenced *FXN* locus. DNA methylation is an important modulator of gene regulation thought to regulate the majority of the human genome. It is possible that this methylation plays a significant role in the etiology of Friedreich Ataxia by virtue of its inverse correlation with *FXN* expression and age of disease start. (Cook e Giunti, 2017)

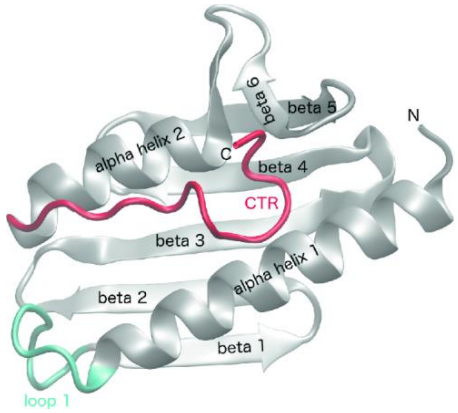

Figure 2 - Frataxin protein structure (Castro et al., 2019)

The diagnosis of Friedreich's Ataxia is based on the clinical features of the patients and also the detection of point mutation or small deletion in the *FXN* gene and/or on the identification of the number of GAA trinucleotide expansion, in the *FXN* greater than 50 repeats both alleles.

1.3. Frontotemporal Lobar Degeneration (FTLD) (OMIM # 600274)

Frontotemporal Lobar degeneration is a clinically heterogeneous insidious degenerative neurological syndrome characterized by progressive deficits in behavior, executive function, and language. It is the second most common form of dementia in all age groups, after Alzheimer's disease. Because of the close resemblance of behavioral changes in patients with Frontotemporal Lobar degeneration to those seen in patients with psychiatric disorders, diagnosis is challenging.(Bang, Spina e Miller, 2015)

1.3.1. Clinical Features

Frontotemporal Lobar Degeneration, is classified into three clinical variants: behavioral frontotemporal dementia, which is associated with early behavioral and executive deficits; primary progressive aphasia non-fluent variant, with progressive deficits in speech, grammar, and word production; and primary progressive aphasia semantic variant, with a progressive disorder of semantic knowledge and naming. The symptoms of all three clinical variants may converge, as the initial focal degeneration becomes more diffuse and spreads to affect large regions in the frontal and temporal lobes. Over time, patients develop global cognitive and motor impairments, including parkinsonism, and motor neuron disease in some of them. Patients with end-stage disease have difficulty eating, moving, and swallowing. Death usually occurs about 8 years after the onset of the first symptoms and is typically caused by pneumonia or other secondary infections (Bang, Spina e Miller, 2015)

1.3.2. Frontotemporal Lobar Degeneration Variants

1.3.2.1. Behavioral Variant

The personality changes, disinhibition, and apathy that characterize behavioral-variant frontotemporal dementia are the most overt early signs. Behavior disinhibition can lead to impolite and socially inappropriate actions (such as approaching strangers without respecting physical and social boundaries), impulsive, new criminal behaviors (such as theft, public urination, sexual advances, or hit-and-run accidents), and embarrassing personal remarks. Reduced inhibition often results in bad fiscal decisions that can lead to financial ruin. Apathy can be misinterpreted for depression since it shows itself as a loss of interest in cleanliness, social interaction, hobbies, and employment. Patients exhibit stereotyped behaviors, such as simple repetitive movements, compulsive ritualistic behaviors, and repetitive verbalizations, as well as a loss of sympathy and empathy for their families and friends, a decrease in social interest and responsiveness to other people's emotions and needs. Different manifestations of hyperorality in frontotemporal behavioral dementia include, increased sweets or alcohol consumption, and weight gain. Patients with behavioral variant frontotemporal dementia often have deficits in several executive tasks, although their visuospatial abilities are quite normal at first, they have little insight into their own behavior and may not recognize many of the changes that are reported by a knowledgeable informant. Some patients have decreased sensitivity to pain (Bang, Spina e Miller, 2015). This variant and its clinical phenotype has been associated with the C_9orf_{72} and *GRN* gene mutation.(Silverman, Goldman e Huey, 2019)

1.3.2.2. Primary Progressive Aphasias

In the early stages of the disease, language abilities gradually deteriorate in patients with primary progressive aphasia. The primary symptom throughout the first two years of the illness is language impairment. Deficits are seen during conversation or through speech and language testing and include language production, object naming, syntax, or word understanding. The primary factor for impaired daily life activities is a language deficit. Primary progressive aphasia can be linked to Alzheimer's disease, even though Frontotemporal Dementia is most frequently the underlying cause. Alzheimer's disease should be taken into consideration if there are significant visual memory problems or visuospatial deficits. The patient should not exhibit behavioral disturbances during the early phase of the disease; such changes are indicative of frontotemporal behavioral dementia variant (Bang, Spina e Miller, 2015). Within primary progressive aphasias there are two groups, fluent variant primary progressive aphasia and nonfluent primary progressive aphasia.

1.3.2.2.1. Fluent Variant Primary Progressive Aphasia

The term semantic dementia has been applied to describe a syndrome characterized by semantic aphasia and associative agnosia. Early asymmetric degeneration of the amygdala and anterior temporal lobes causes the symptoms. Semantic loss results in abnormalities in people, places, and things, problems finding words, and problems understanding words. While the right temporal lobe variation mostly manifests as behavioral alterations, the left temporal lobe variant primarily manifests as linguistic semantic loss (primary semantic-variant progressive aphasia). About three times as many people have the left temporal lobe variant than the right temporal lobe variant. Deficits in recognizing objects and people go beyond the visual domain, and tactile, olfactory, or gustatory do not help. As the disease spreads from the temporal lobes to the orbitofrontal cortex, behavioral changes occur, such as irritability, emotional withdrawal, insomnia, and strict or selective eating. Although semantics are lost in the left temporal lobe variant, functions related to the right side, such as visual attention, are sometimes accentuated. As a result, people who have the left temporal lobe variation often grow compelled to look at certain things. Patients with the right temporal lobe variety, on the other hand, grow verbal compulsions that involve both words and symbols (Bang, Spina e Miller, 2015)

1.3.2.2.2. Nonfluent Primary Progressive Aphasia

Primary progressive aphasia nonfluent variant is characterized by slow, labored and halting production of speech, and by omission or incorrect use of grammar (agrammatism).

Patients frequently make inconsistent sound errors in speech, including insertions, deletions, substitutions, transpositions, and distortions. Patients may have difficulty understanding sentences with complex syntactic constructions, but retain the ability to understand simpler sentences with the same semantic content. Early in the disease, written language production and syntactic comprehension tests reveal slight grammatical errors. Some patients maintain intact writing despite the presence of marked deficits in spoken language. Single-word comprehension and object knowledge are not affected, although patients may have a mild abnormality that is usually more pronounced for verbs than for nouns.(Bang, Spina e Miller, 2015)

1.3.3. Genetics

A family history of dementia is described in up to 40% of frontotemporal lobar degeneration cases, although a clearly autosomal dominant history accounts for only 10% of cases. Autosome dominant mutations in the *C9orf72*, *MAPT*, and *GRN* genes account for about 60% of all cases of hereditary frontotemporal lobar degeneration. The *C9orf72* gene mutations account for about 25% of familial cases of frontotemporal lobar degeneration and are the most common genetic cause of frontotemporal lobar degeneration and amyotrophic lateral sclerosis. The mutation is a hexanucleotide repeat, G_4C_2, in a non-coding region of *C9orf72*. (Olney, Spina e Miller, 2017) *MAPT* and *GRN* mutations each account for 5–20% of familial frontotemporal lobar degeneration cases. The *MAPT* mutations, which were the first single monogenic cause of hereditary frontotemporal lobar degeneration to be identified, promote neurodegeneration by stabilizing altered microtubules and facilitating tau's propensity to assemble. On the other hand, *GRN* mutations are associated with haploinsufficiency and a loss of the functional progranulin levels in serum and cerebral fluid. Progranulin, a secreted protein involved in cell cycle regulation, wound healing, axonal growth, and inflammation modulation, may compete with TNF-induced inflammation. It binds to the tumor necrosis factor (TNF) receptor(Bang, Spina e Miller, 2015). The exact role of *C9orf72* is still being studied, but this expansion is thought to cause a loss of function in transcription, as well as possible gain of function due to toxic RNA foci. Dipeptides are produced by the abnormal expansions that probably also contribute to neurodegeneration. The *C9orf72* protein is expressed mostly in the brain, spinal cord, and immune system, and at lower levels in other organs (lung, heart, liver, kidney, and skeletal muscle) (Smeyers, Banchi e Latouche, 2021). The figure 3 show the structure of the *C9orf72* gene.

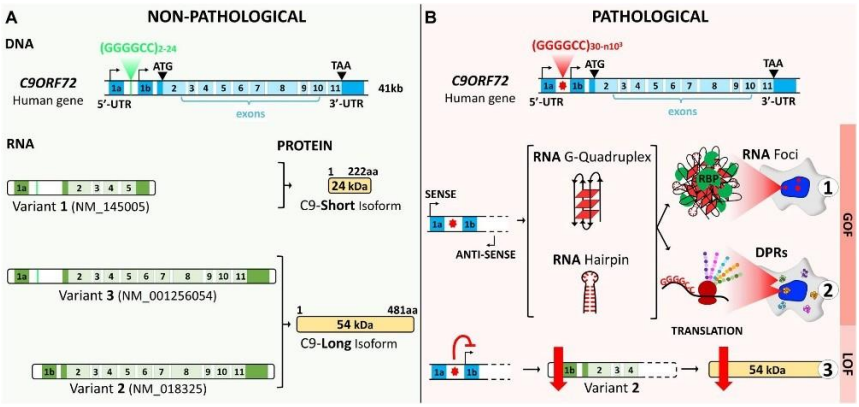

Figure 3- The structure of the *C9orf72* gene, transcript variants and protein isoforms under a non-pathological (A) and pathological (B) state. (A) The human *C9orf72* locus includes two non-coding exons (1a and 1b), light blue, and 10 coding exons (2-11), dark blue. Giving rise to three coding variants: variant 1, V1, which includes exon 1a and exons 2-5; variant 2, V2, which includes exon 1b and exons 2-11; and variant 3, V3, which includes exon 1a and exons 2-11. (B) In a pathological state, the G_4C_2 repeat located between the two non-coding exons (1a and 1b) is abnormally expanded. Bidirectional transcription of hexanucleotide repeat expansion (HRE) generates G_4C_2 sense and G_2C_4 anti-sense expanded RNAs. These HRE transcripts give rise to G-quadruplex and hairpin structures that can form RNA foci and sequester RNA-binding proteins (RBP) (B1). The expanded RNAs are also translated via non-ATG (RAN) repeat-associated translation, resulting in the synthesis of dipeptide protein repeats (DPRs) (B2). Finally, the presence of HRE inhibits transcription, leading to a decrease in *C9orf72* protein (B3). (Smeyers, Banchi e Latouche, 2021)

The molecular diagnosis of Frontotemporal Lobar Degeneration is performed with detection of the number of G_4C_2 repeat expansions in the *C9orf72* gene (>30 repeats) and also with detection of pathogenic mutations in the *GRN* gene and *MAPT* gene.

1.4. Amyotrophic Lateral Sclerosis (OMIM # 105550)

Amyotrophic Lateral Sclerosis (ALS) was originally defined as a pure motor neuron disease by Jean-Martin Charcot in 1869. Today it is known as a multisystemic neurodegenerative disease, with clinical, genetic and neuropathological heterogeneity. (Masrori e Damme, Van, 2020). The mean age of onset of ALS varies from 50 to 65 years with the median age of onset of 64 years old. Only 5% of the cases have an onset <30 years of age.

1.4.1. Clinical features

The clinical presentation of ALS typically consists of adult-onset focal muscle weakness and wasting, which has a tendency to spread with disease progression. The weakness begins most often in the limb muscles, more often in the distal muscles than in the proximal muscles. In about 25%-30% of cases there is a bulbar onset of the disease, presenting with dysarthria, dysphagia, dysphonia, or more rarely with masseter weakness. There is a high degree of variability in the age of onset, the site of onset, and the rate of progression of ALS disease.

The disease is relentlessly progressive in most patients, with a median survival of about 3 years after the onset of symptoms, where death is mainly attributed to respiratory failure. About 50% of patients will suffer from extra-motor manifestations to some extent, in addition to their motor problems. (Masrori e Damme, Van, 2020)

1.4.2. Genetics

At the genetic level there is also considerable heterogeneity of disease, with more than 20 genes that have been associated with ALS. The five most common genetic causes are hexanucleotide expansions on C_9orf_{72} and mutations in *SOD1*, *TARDBP*, *FUS* and *TBK1*. Together, they explain about 15% of all patients. The most common neuropathological signature of ALS is cytoplasmic aggregation of TDP-43, a protein encoded by *TARDBP*, which is found in more than 95% of the ALS case. TDP-43 inclusions are not unique to patients with mutations in *TARDBP,* but are also present in patients with C_9orf_{72} expansions or *TBK1* mutations and in patients with sporadic ALS (sALS). TDP-43 is predominantly localized in the nucleus under basal conditions, but in ALS it moves to the cytoplasm to form aggregates and become phosphorylated. Other aggregating proteins, such as *SOD1* and *FUS*, are found in patients with *SOD1* and *FUS* mutations, respectively. Patients with C_9orf_{72} hexanucleotide repeat expansions have accumulations of dipeptide repeat proteins that are translated from G_4C_2 repeats. (Masrori e Damme, Van, 2020).

The molecular diagnosis of ALS is made by detecting point mutations one of the genes associated with ALS and in the detection of G_4C_2 repeat expansions in the C_9orf_{72} gene (> 30 repeats).

1.5. Huntington's Disease (OMIM #143100)

Huntington's disease is a progressive brain autosomal dominant disease, caused by an expansion of a CAG trinucleotide repeat encoding in exon 1 of the *huntingtin (HTT)* gene. It usually manifests in adulthood, after a pre-symptomatic life stage of years, depending on the penetrance of the CAG mutation, which affects the corticostriatal connections with dysfunction and loss of brain cells (Luca, De *et al.*, 2021). The prevalence of HD, an uncommon condition, is 10–12 people per 100,000 people of European ancestry. The number of repetitions in *HTT* is inversely associated with disease onset, so that the higher the number, the earlier the onset (Nopoulos *,* 2016). The adult onset of this disease, which typically strikes people in their thirties or forties, is the most prevalent kind. Adult-onset HD patients typically survive 15 to 20 years after the first indications and symptoms appear. Juvenile-onset Huntington's disease, is a less prevalent variant of the illness, first manifests in youth or

adolescence. Individuals with this type of the disease often live 10 to 15 years following the onset of signs and symptoms; it tends to advance more quickly than the adult variant.

1.5.1. Juvenil HD (JHD)

The Huntington's disease is associated with the phenomenon of anticipation, that is, the process by which the clinical manifestation appears at an earlier age and/or becomes more severe as the spread is passed on from generation to generation (Depienne e Mandel, 2021).

Longer *HTT* expansions cause early onset of the disease. When this occurs before the age of 21, it is referred to as JHD. This type of Huntington's disease shares many characteristics with adult-onset HD, including a propensity for motor, cognitive, and mental symptoms. The presentation and predominance of motor symptoms, however, varies noticeably in adult-onset HD, with chorea/hyperkinetic symptoms first and hypokinetic symptoms afterwards. The motor presentation of JHD is typically hypokinetic with bradykinesia, stiffness, and dystonia and can subsequently progress to hyperkinetic behavior. Seizures are another affliction that comes with JHD. Seizures can be severe and challenging to manage, and they are most frequent in children with JHD (diagnosed before age 10). Although the cognitive alterations in JHD are progressive, they can also have an impact on children's capacity to learn and acquire abilities prior to the deterioration of those skills. Of the symptoms of JHD, the psychiatric and behavioral symptoms are much more consistent and prominent. That is, the majority of patients will have behavioral symptoms. These symptoms are composed almost exclusively of externalizing behaviors of hyperactivity, impulsivity, poor mood regulation, irritability, and angry outbursts. Although there is a perception that patients with JHD may have a more rapid course of the disease than those with onset in adulthood, the literature presents conflicting reports, leaving a question that has not yet been fully explored (Nopoulos, 2016).

1.5.2. Clinical Features

The clinical symptoms of HD are defined in three domains: motor, cognitive, and psychiatric. Motor symptoms are progressive and at the onset of the disease, are mainly hyperkinetic with involuntary chorea movements. These movements usually start out longer and of a small degree, then become more systematic and of greater amplitude. These movements are often incorporated into the natural voluntary movements, and so at first may appear to be simple restlessness. Although the early stages of motor symptoms are hyperkinetic, in the later stages of the disease, motor symptoms tend to be hypokinetic with bradykinesia and dystonia. The inability to move freely and irregular eye movements are additional classic symptoms. Dysphagia develops into a symptom with high morbid effect as

the disease progresses because aspiration and pneumonia are common causes of death. The cognitive dysfunction occurs in the vast majority of patients. In the early stages, this may be somewhat limited to executive function, with difficulties in decision making, organization, planning, and multitasking. Eventually, when these conditions deteriorates, a more comprehensive picture of cognitive abnormalities and a dementia diagnosis become clear. Although the psychological symptoms of HD can vary, the majority of them are consistent with frontal lobe dysfunction, which is compatible with the pathophysiology of the disease as it is currently understood. These symptoms, which include poor mood regulation, impulsivity, impatience, and inattention, are initially associated with frontal disinhibition. Family members typically think of these symptoms as a personality change in the early stages of the disease. Anger and aggressiveness can be expressed as a result of HD's extreme irritability. After the disease, symptoms usually take on more of a frontal constellation of symptoms, with prominent apathy or loss of initiative, creativity, and curiosity. This is accompanied by a generalized emotional blindness. Family members often interpret these symptoms as depression, and objectively, the patient certainly seems more withdrawn, disinterested, and non-interactive. However, subjectively, patients deny any feelings of sadness or hopelessness and usually describe their mood as good or fine. Apathy is usually the most common feature of the disease, occurring at the highest prevalence and is progressive, along with other progressive features such as motor symptoms and cognitive decline. The depression is a characteristic often described to be associated with HD. However, what is not clear is whether depressive symptoms are a manifestation of the disease process with direct links to the neurological underpinnings of the pathology. Given the course of a degenerative disease, any associated symptoms that are present early in the disease course but diminish over time suggest that it is not the underlying pathology that drives depressive symptoms. Despite the depressive symptoms in HD, treatment of these symptoms and the need for careful screening for suicide risk remain a vital part of care for this patient population. A prominent feature of HD is lack of awareness or lack of perception of the nature or severity of the symptoms the patient is experiencing. This can include lack of awareness of any feature of the illness, including the three domains of motor, cognitive or behavioral symptoms. Due to this quality, it is necessary to take into account family members as valuable (and occasionally essential) sources of information who offer unbiased assessments of the patient's symptoms and level of function and who should be involved in the patient's health assessments and decision-making (Nopoulos, 2016)

1.5.3. Genetics

The mutation responsible for Huntington's disease, is caused by an unstable expansion of CAG trinucleotide repeats located at the 5' end of exon 1 of the *HTT* gene. The huntingtin protein is expressed in all human cells although with highest concentration in brain tissue. Lower concentrations exist in the liver, heart and lungs (Januario *et al,* 2011). Mutation in this gene results in neuronal dysfunction and death through various mechanisms. These include direct effects of the mHTT (mutant huntingtin) fragment in exon 1, the propensity of mHTT to form abnormal aggregates, and its effects on cellular proteostasis, axonal transport, transcription, translation, mitochondrial and synaptic function (McColgan e Tabrizi, 2018). The *HTT* gene is translated into full-length huntingtin protein as well as an amino-terminal *HTT* exon 1 fragment (the result of aberrant splicing). The figure 4 show the cellular pathogenic mechanisms in Huntington's disease.

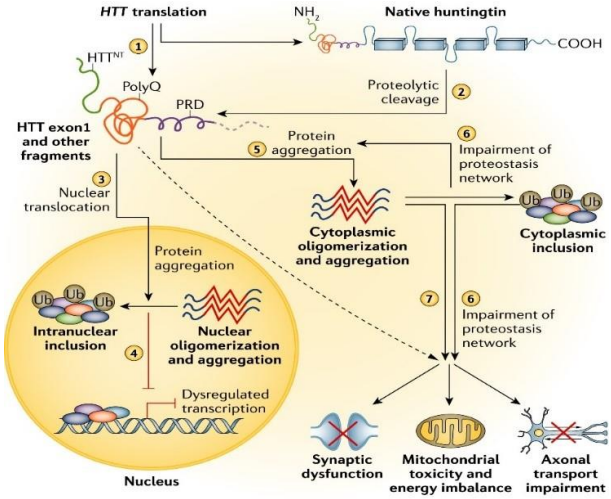

Figure 4- Pathogenic cellular mechanisms in Huntington's disease. (1) *HTT* is translated to produce the full-length Huntington's protein as well as an amino-terminal fragment of *HTT* exon 1. The polyglutamine (polyQ) tract length. (2) The native full-length Huntingtin is cleaved through proteolysis to generate additional protein fragments. (3) The protein fragments enter the nucleus. (4) The fragments are retained in the nucleus through self-association and aggregation. (5) Huntingtin fragments oligomerize and aggregate in the cytoplasm. (6) Huntingtin aggregation is exacerbated through disease-related deterioration of the proteostasis network, which also leads to global cellular impairments. (7) Aberrant forms of huntingtin result in additional global cellular impairments, including synaptic dysfunction, mitochondrial toxicity, and a decreased axonal transport rate. (McColgan e Tabrizi, 2018)

The molecular diagnosis of Huntington's disease is made by detecting of expanded CAG repeats in exon 1 of the *HTT* gene, (>40 repeats).

1.6. Machado Joseph Disease (MJD) (OMIM # 109150)

Machado-Joseph disease, also referred to as spinocerebellar ataxia type 3 (SCA3), is the worldwide most common form of SCA. MJD is a dominant neurodegenerative disease of

late onset that predominantly involves the cerebellar, pyramidal, extrapyramidal, motor neuron, and oculomotor systems; although it shares features with other SCAs, the identification of smaller but more specific signs facilitates its differential diagnosis. This disease is currently considered the most common form of SCA globally. The average age of onset is around 40 years, with extremes of 4 and 70 years, and has an average survival of 21 years (ranging from 7 to 29 years) (Bettencourt e Lima, 2011). Since the discovery, that MJD mutation has been linked to hereditary ataxia in a number of different ethnic groups. MJD is the most prevalent autosomal dominant ataxia in various parts of the world, including Portugal. The extent of the expansion corresponds inversely with the age of symptom onset in all diseases brought on by expansions. Larger repeats, on average, result with earlier disease onset and may be linked to a faster rate of disease development. The clinical characteristics indicated above are also partially determined by the amount of the extent of the enlarged repeat (Paulson, 2018).

1.6.1. Clinical Features

Machado Joseph Disease is associated with the phenomenon of anticipation, i.e., the tendency for repeat sizes to expand from generation to generation, together with the fact that longer repeats cause earlier onset disease, leads to disease symptoms appearing earlier in successive generations. Over half of the parent-child transmissions of the MJD repeat are unstable, with ~ 75% expanding further in the next generation, appear to be slightly more prominent with paternal than maternal inheritance. The primary clinical symptom of MJD is increasing ataxia brought on by brainstem and cerebellar dysfunction. But ataxia never happens by itself. The brainstem, oculomotor system, pyramidal and extrapyramidal pathways, lower motor neurons, and peripheral nerves are just a few clinical issues that exhibit progressive dysfunction. Patients with severe dysarthria and dysphagia and wheelchair use are signs of an advanced disease. Additionally, patients may experience amyotrophy, dystonia, spasticity, and temporal and facial atrophy. Survival after the onset of the disease ranges from ~20 to 25 years. The variability concerning the age of disease onset, reflects differences in repeat size: larger repeats cause earlier disease on average. For the same reason, the phenotype of MJD can vary markedly.(Paulson, 2018) Based on this diversity, there are various clinical forms of MJD. Type I disease has an earlier onset (approximately 25 years on average) and is distinguished by bradykinesia and little ataxia. The most prevalent form of the disease, Type II disease, starts in young to middle age and is characterized by upper motor neuron symptoms and progressive ataxia. Type III is characterized by ataxia, substantial peripheral nerve involvement, generalized amyotrophy, and areflexia, and has a late onset (mean age of onset

50 years). There is a type IV variant of the illness that is marked by parkinsonism, according to some researchers. (Lin *et al.*, 2018) Patients with type I disease, the early onset dystonic form of the disease, typically have longer repeats than those with type II, type III and type IV phenotypes. Larger CAG repeats are often associated with pyramidal signs and dystonia. (Paulson, 2018)

1.6.2. Genetic

The cause of Machado Joseph disease, is an unstable CAG repeat expansion mutation in the coding region of the *ATXN3* gene. This gene, which has 11 exons, encodes the disease protein ataxin-3. The $ATXN_3$ gene encodes ataxin-3, a 42-kDa protein that is widely expressed in the CNS and elsewhere. The CAG repeat resides in the 10th exon, where it encodes a polyglutamine tract. This protein exists in at least two major splice forms that differ only in their carboxyl-terminial. Both contain the polyglutamine domain encoded by exon 10 and both appear to be expressed in the disease brain. The protein ataxin-3 is small soluble protein that can move in and out of the nucleus. In many cells, a fraction of the cellular pool of ataxin-3 is intranuclear, bound to the nuclear matrix. In the brains of unaffected individuals and in normal neurons, ataxin-3 appears to be largely cytoplasmic. In the brains of individuals with the disease, the protein tends to concentrate in the neuronal cell nucleic. Ataxin-3 localizes preferentially in the nucleic of neuronal cells in the disease, but this same phenomenon has been described in other polyglutamine diseases, including Huntington's disease.(Paulson, 2018)

The diagnosis of Machado Joseph disease is based on the detection of the CAG trinucleotide repeat expansions, in the *ATXN3* gene, (>53 repeats).

1.7. Objectives

The main aim of this project was the genetic characterization of patients with repeat expansion disorders, such as: Friedreich's Ataxia, Frontotemporal Lobar Degeneration, Amyotrophic Lateral Sclerosis, Huntington's disease and Machado Joseph disease.

The specific objectives outlined were:

1) To set up different molecular techniques to detect the pathological expansions in these patients;
2) To quantify the number of DNA repeats in the different patients;
3) To optimize the mutations analysis in the *FXN* gene;
4) To establish genotype- phenotype correlations.

2.1. Study Population

All the participants in this study were recruited at the Neurology Department of the Coimbra University Hospital. This study included 42 patients with the clinical diagnosis of Frontotemporal Lobar Degeneration and/or Amyotrophic Lateral Sclerosis. Also, 14 relatives who were still asymptomatic were included. For this last group, an informed consent was required in the context of genetic counselling. In addition, patients with the clinical diagnosis of Friedreich's Ataxia (n=10), Huntington's Disease (n=10) and Machado Joseph Disease (n=16), were recruited.

Whole Blood samples from each individual was collected (two 3 mL tubes with EDTA), which were stored at 4°C for further DNA extraction.

2.2. DNA Extraction

The Genomic DNA was extracted from the blood samples by the NZY Tissue gDNA Isolation ® kit (Nzytech, Lisbon, Portugal), according to the manufacturer's instructions. The NZY Tissue Isolation kit is designed for the simple and rapid small-scale preparation of highly pure genomic DNA from a variety of sample sources (e.g., whole blood, serum, plasms, or body fluids). This kit uses optimized lysis buffers containing Proteinase K and SDS to release DNA from cells. After preparing the lysate, DNA was selectively absorbed into the NZYSpin Tissue Colum and other impurities such as proteins and salts were removed during the washing steps. The DNA was eluted with 100 uL of Buffer.

2.3. DNA Quantification and Quality control

The DNA concentration [ng/µL] and quality control was calculated using, the NanoDrop ND-1000 Spectrophotometer (Thermo Fisher Scientific USA), version 3.5.2 and its software, which was based on spectrophotometry. The DNA readings were taken at wavelengths of 260 nm and 280 nm, which allows the nucleic acid concentration (ng/µL) to be calculated, using the lamber beer law. Generally, the ratio of nucleic acid to protein (260/280), is used to check the purity of DNA samples.

2.4. Analysis of *FXN* gene by Sanger Sequencing

2.4.1. DNA Amplification by PCR (Polymerase Chain Reaction)

The DNA amplification was performed using the PCR technique, in which the primers were previously designed for each exon in the laboratory, where it was necessary to use the ENSEMBL (ensembl.org) database to find reference sequence of the respective gene, the HUGO database (https://www.genenames.org/), the Primer 3 plus (https://www.bioinformatics.nl/cgi-bin/primer3plus/primer3plus.cgi) software and Oligocalc (http://biotools.nubic.northwestern.edu/OligoCalc.html) platform to design and to confirm the specificity of the primers selected. Tables 1 shows the sequence of the primers and the length of the respective amplify product.

Table 1- Primer Sequence, and PCR Size of exon 1,2,3,4, and 5 of the *FXN* gene

Name	Sequence (5´-3')	PCR size (bp)
FXN-Ex1F	CTGCTCCCCCACAGAAGAGT	396
FXN-Ex1R	AGGAGCGGGGTGAGCTAGT	
FXN-Ex2F	GGCACTCGAATGTAGAAGTAGCA	250
FXN-Ex2R	AGAGGCAGGGAAGGAGAGAG	
FXN-Ex3F	TGGAAGCATTTGGTAATCATGT	248
FXN-Ex3R	TCTTAGAGGGGGAAACAGAAAA	
FXN-Ex4F	GAAGCAATGATGACAAAGTGC	232
FXN-Ex4R	TGTCACATTTCGGAAGTCTTT	
FXN-Ex5F	GCAGCATTTGTGGAATCAGT	284
FXN-Ex5R	TAATGAAGCTGGGGTCTTGG	

The mixture reagents to amplify of *FXN* region by PCR reaction was prepared for a final volume 25 uL, according to the table 2.

Table 2- Reagent used in the PCR mixture to amplify *FXN* gene

Reagent	Final Concentration	Volume (µL)
H_20	-	14.4
Taq Buffer 5x (Promega)	1x	5
dNTPs 5mM	0.2 mM	1
MgCl2 (25 mM) (Promega)	1.5 mM	1.5

Primer Foward 10 mM	0.5 µM	1
Primer Reverve 10 mM	0.5 µM	1
Taq DNA polymerase Promega (uL/5U)	0.5 U	0.1
Total		24

All PCR reagents, we pipetted into a 0.2 mL PCR tube according to Table 2. Then 1 µL of DNA (100-150 ng/ µL) was added into the respective tubes for the final volume of 25 µL. All PCR reactions performed included a negative control, and were placed in the Biometra thermal cycler. The amplification of exon 1 follows the conditions that are represented in Table 3. While the amplification conditions of the remaining exons (2-5), follow the conditions that are represented in table 4.

Table 3- The exon 1 amplification conditions

Steps	Temperature (°C)	Time	Cycles
Initial Denaturation	96	5 min	1
Denaturation	94	45 sec	30 x
Primers	66	45 sec	
DNA extension	72	45 sec	
Final Extension	72	10 min	1
Cooling	4	∞	1

Table 4- The exon 2,3,4 and 5 amplification conditions

Steps	Temperature (°C)	Time	Cycles
Initial Denaturation	96	2 min	1 x
Denaturation	94	30 sec	14 x
Primers	60	30 sec	
DNA extension	72	30 sec	
Denaturation	94	30 sec	9 x
Primers	55	30 sec	
DNA extension	72	30 sec	
Denaturation	94	30 sec	9 x
Primers	50	30 sec	

DNA extension	72	30 sec	
Final Extension	72	10 min	1 x
Cooling	4	∞	

2.4.2. Electrophoresis in Agarose Gel

The results of the PCR products were confirmed by an agarose gel electrophoresis run. The samples were loaded onto a 2% concentration agarose gel plate with 6 uL of GreenSafe Premium (NZYtech) and exposed to an electric field, by a power supply at 100 volts. Each sample batch's corresponding negative control was loaded beside it. Once electrophoresis finished, a photograph was taken using UV transilluminator (BIO RAD Molecular Imager® ChemiDoc™ XRS+ Imaging System), with the software Quantity One version 4.6.9.

2.4.3. Purification of PCR Products

After, the PCR products were purified to remove salts, dNTPs, primers and polymerases which have not been incorporated during the PCR reaction. We used the Exo/SAP Go PCR Purification Kit, with the enzymes exonuclease I (EXO) and shrimp alkaline phosphatase (SAP), to enzymatically purify the PCR reaction. Samples were placed into Biometra thermal cyclers, according to the conditions listed in table 5.

Table 5- Conditions for purification of PCR products by EXO/SAP Go PCR Purification Kit

Steps	Temperature (°C)	Time (min)
Incubate	37	5
Heat Inactivate	80	10
Cooling	4	∞

2.4.4. Sequencing Reactions

The direct sequencing reaction, based on Sanger Sequencing, using the GenomeLab™ DTCS with Quick Start Kit (Beckman Coulter) was prepared. This kit has a master mix which contains DNA polymerase, dNTPs dye terminators (ddUTP, ddGTP, ddCTP and ddATP) and reaction buffer. During a sequencing reaction, the dNTPs and ddNTPs were incorporated on the 3' end of DNA strand by DNA polymerase. Every time that one ddNTP is added to the DNA strand, the elongation is finished. Thus, several DNA molecules with different size and

bases were generated. Each reaction was prepared in a 0.2 mL tube using just one primer. After tubes identification, the sequencing reactions were prepared for a final volume of 20 uL adding all components listed in table 6. After preparing the sequencing reactions, all tubes were briefly vortex to mix all components before placed in Biometra thermocycler, according to the following conditions described in table 7:

Table 6- Reagents used in sequencing reactions

Reagent	Volume (µL)
DTCS Quick Start Master Mix	3
Primer (10 pmol/uL) (Fwd or Rev)	1
DNA template	0.5- 10[1]
dH_2O (adjust total volume to 20.0 µL)	6-15.5
Total	20

1- The DNA added was defined taken into account the band intensity observed in the agarose gel.

Table 7- Conditions of sequencing reaction on thermocycler

Temperature (°C)	Time	Cycles
96	20 s	30x
50	20 s	
60	4 min	
4	∞	

2.4.5. Purification of Sequencing Reaction Products

The products resulting from the sequencing reactions were immediately purified in order to remove any residual salts, ddNTPs and other components that were not incorporated during the reaction and could interfere with the sequence analysis. The purification of sequencing reactions was based on ethanol precipitation. A mixture of 62.5 µL ethanol (95%), 3 µL of NaOAc (3M) and 14.5 µL ddH_2O, was added to each sample, in a 96-well PCR plate, that was sealed with Parafilm and Stored at -20°C for 10 min. Three consecutive centrifugations were performed, in the Allegra TM 25R Centrifuge at 5700 rpm (Beckman Coulter), one lasting 30 minutes, 10 minutes and lastly 5 minutes and between them

the supernatant was discarded and cold 70% ethanol (-20°C) was added to each well. At the end, the pellets were resuspended in 25 uL Formamide (provided in the kit) by vortex.

2.4.6. Analysis and Interpretation of Sequencing Results

The product of the sequencing readings was separated by eight capillary electrophoresis using a CEQ 8000 Genetic Analysis System automated sequencer (Beckman Couter). Base calling was accomplished using four spectrum channels of laser-induced fluorescence, each of which targeted a different fluorochrome.

Sequence read files were exported as electropherograms and further analyzed on demo version of the SEQUENCER ™ software. The electropherograms were manually analyzed by two independent operators by comparison with the reference *FXN* gene sequence (GenBank accession: NM_000144.5).

2.5. Detection of the GAA trinucleotide repeat expansion in the *FXN* gene

The detection of GAA repeat expansions in the *FXN* gene was performed using the Adellgene Friedreich's Ataxia ™ (Diagnostica Longwood, Zaragoza, Spain). Kit for the determination by fluorescent fragment analysis of the presence of healthy, premutated and mutant alleles in this gene. The kit technology was based on the PCR of genomic DNA extracted and purified from peripheral blood, followed by fluorescence analysis of the size of the PCR fragments obtained by the genetic analyzer and conversion of that size in the number of GAA repeats. The kit has two Primer Mixes (PM): Primer Mix 1, is design to perform PCR, for amplification of all samples, detecting heterozygous and possible homozygous alleles with a size below 200 GAA repeats; and Primer Mix 2, is design to perform TP-PCR, for confirmation of homozygous samples and detection of expansion alleles with a size >200 GAA repeats.

2.5.1. PCR Reactions Preparation

PCR uses two primers, one of which is fluorescently labeled for later detection on the sequencer. We pipetted all reagents from the Adellgene Friedreich's Ataxia kit into 0.2 mL and prepared a mixture containing 4.3 µL of the AD-FA-PM_1 and 18.7 µL of the AD-FA-POM_1. Then 1 µL of DNA (50 ng/ µL) was added into the respective tubes for the final volume of 23 µL. All PCR reactions performed included a negative control and were placed in the Biometra thermal cycler. The table 8 shows the conditions of amplification.

Table 8- Conditions of the Adellgene Friedreich´s Ataxia Kit

Steps	Temperature(°C)	Time	Cycles
Denaturation	98°C	5 min	1 x
Cycles	97°C	45 sec	35 X
	64°C	45 sec	
	68°C	3 min+ 10 sec/cycle	
Final Extension	72°C	30 min	1 x
Cooling	4°C	∞	

2.5.2. Electrophoresis in Agarose Gel

Confirmation of the amplification products was done by an agarose gel electrophoresis run. This was prepared according to the procedure described in section 2.4.2.

2.5.3. Preparation of the samples for capillary electrophoresis

To perform the capillary electrophoresis analysis, it was necessary to prepare a mixture containing formamide, which was used to resuspend samples prior to electrokinetic injection into capillary electrophoresis systems, and the internal lane size standard ROX 1000, which allows automated data analysis and accurate DNA fragment size comparisons between electrophoresis runs. We pipetted into each well of a 96 well plate, 10 uL of Hi-Di ™ Formamide (Applied Biosystems, Foster City, CA, EUA) and 1 uL of ROX 1000 Size Ladder (Diagnostica Longwood, Zaragoza, Spain) a total of 11 uL. Then we added 1 µL of previously prepared PCR product, diluted 1:100. After that, the plate was pulsed in the plate centrifuge, in Allegra ™ 25R Centrifuge (Beckman Coulter), and the samples was denatured for 2 minutes at 95°C, and then put on ice for about 5 minutes, before loaded in the 3130 genetic analyzer.

2.5.4. Analysis and Interpretation of Results

Sequence reading was performed on the 3130 genetic analyzer (Applied Biosystems, Foster City, CA, USA) according to the conditions of the protocol. Fragments were separated by 4 capillary electrophoresis, which used a POP-7 polymer separation matrix for fragment analysis. The products were separated by size based on their total charge. Since each dye emits light at a different wavelength when excited by the laser, all colors, and therefore loci, can be detected and distinguished in a single capillary injection. The FSA files were exported as electropherograms and were analyzed by Gene Mapper software (Thermo Fisher Scientific,USA) version 3.7. The electropherograms were analyzed by independent operators

and samples with two peaks were heterozygous, one peak we considered homozygous. All homozygous samples were further analyzed as described in sections 2.5.5.

To quantify the number of GAA repeat expansions, we use the values given in the protocol concerning the correlation between the size fragments and number of GAA repeats. The size of each peak may be converted to repeat length according to the Equation below:

$$(GAA)n = \frac{Peakn - Co}{mo}$$

where, Peakn is the size in base pairs of a given gene-specific product peak, Co is the Size Correction Factor (i.e. Intercept (b)) and mo is the Mobility Correction Factor (i.e. Slope (a)) extracted from the linear calibration curve (y=ax+b).

2.5.5. TP-PCR Reactions Preparation

Triplet primed PCR (TP-PCR) was used according to Adellgene Friedreich's Ataxia kit protocol. A mixture containing 8.8 µL of the AD-FA-PM_2 and 18.7 µL of the AD-FA-POM_2., was prepared. Then 1 µL of DNA (50 ng/ µL) was added into the respective tubes. All TP-PCR reactions performed included a negative control and were placed in the thermal cycler. The conditions for the TP-PCR in the Biometra Thermal Cycler were previously described in section 2.5.1.

2.5.6. Purification of the TP- PCR products

TP-PCR products were purified to remove salts, dNTPs, primers and polymerases which have not been incorporated during TP-PCR reaction. 18 uL of the TP-PCR reactions was added, 500 uL of Capture buffer (provided by the kit) in a 1.5 mL tube. Three centrifugations were made in the Sigma 1-15 centrifuge at 16000g, two lasting 30 seconds and one taking 1 minute, between them supernatant was discarded. In the second centrifugation we added 500 µL of wash buffer (provide by kit) and in the last one, 18 µL of elution buffer and was added to elute it be the purified TP-PCR products.

2.5.7. Preparation of the samples for capillary electrophoresis

The preparation of the TP-PCR samples for capillary electrophoresis were according to section 2.5.3. However, we pipetted 1 uL of the purified TP-PCR product to each well plate.

2.5.8. Analysis and Interpretation of Results

The resulting electropherogram of TP-PCR showed the full-length PCR products generated from the GAA repeat primed peaks. These peaks are separated by 3 bp. A decrease peak's saw along the electropherogram corresponded to a >200 GAA repeats.

2.6. Detection of the G_4C_2 repeat expansion in the *C9orf72* gene

The detection of G_4C_2 hexanucleotide repeat expansions in intron 1 of the *C9orf72* gene was performed using the Asuragen Amplidex® PCR/CE *C9orf72* kit (Austin TX, USA). This kit was used to amplify the hexanucleotide fragment *C9orf72* of purified genomic DNA using a three-primer G_4C_2-Repeat Primed (RP)-PCR configuration, followed by fragment analysis on an Applied Biosystems Genetic Analyzer (3500 Genetic Analyzer, Applied Biosystems, Foster City, CA, USA). The size of the RP-PCR products was converted to the number of G_4C_2 repeats using size and mobility conversion factors. The kit provided a PCR control comprised at 4 normal alleles (2, 5, 8 and 10 G_4C_2 repeats).

2.6.1. RP-PCR Reactions Preparation

The G_4C_2 RP-PCR, uses three primers, two gene-specific primers and a third PCR primer that is complementary to the *C9orf72* hexanucleotide repeat region. We pipetted all reagents from the Amplidex PCR/CE *C9orf72* kit in a final volume of 13 µL, according to table 9. Then 2 µL of DNA (5 ng/ µL) was added into the respective tubes. All RP- PCR reactions performed had included a negative control. The table 10 shows the conditions of the RP-PCR master mix.

Table 9-The reagents used in the RP-PCR

Reagents	Volume (uL)
GC-Rich Amp Buffer	11,45
GC-Rich Amp Buffer	0,5
C9orf72 Repeat Primer	0,5
Diluent	0,5
GC-Rich Polymerase Mix	0,05
Total	13

Table 10- Conditions of the amplifications

Temperature(°C)	Time	Cycles
98°C	5 min	1 x
97°C	35 sec	37 X
62°C	35 sec	
72°C	3 min	
72°C	10 min	1 x
4°C	∞	

2.6.2. Preparation of the samples for capillary electrophoresis

The preparation of the RP-PCR samples for capillary electrophoresis were according to the section 2.5.3. However, we pipetted 12 uL of Formamide and 2 uL of ROX 1000, and 1 uL of RP-PCR product.

2.6.3. Analysis and Interpretation of Results

The sequence reading was performed on 3500 Genetic Analyzer (Applied Biosystems, Foster City, CA, USA), according to the conditions in the Asuragen Amplidex PCR/CE C_9orf_{72} kit protocol, where the fragments were separated by 8 capillary electrophoresis, with a POP-7 polymer separation matrix for fragment analysis. The FSA files were exported as electropherograms and then were analyzed by Asuragen Amplidex® PCR/CE Reporter program (Austin TX, USA) version 3.0. The electropherograms were analyzed by two independent operators to quantify the number of repeats G_4C_2 we used 3 different methods: i) the AmplideX_PCR_CE, where the software gives us the number of G_4C_2 repeat expansion automatically, ii) through the proposed correction factors for 3500 Genetic Analyzer (Co=117,7 and mo=5,8), and iii) according to the established linear calibration curve generated by the 4 peaks of known repeat lengths of the PCR control sample provided by the kit. The size of the peaks of the samples were converted to repeat length according to the equation previously described in section 2.5.4.

2.7. Detection of the CAG trinucleotide repeat expansion in the *HTT* gene

The detection of the CAG trinucleotide repeat expansion in exon 1 of the *HTT* gene was performed using the Asuragen Amplidex®PCR/CE *HTT* kit (Austin TX, USA). This kit was

used to amplify the *HTT* trinucleotide CAG fragment from purified genomic DNA. The amplified products were resolved by a capillary electrophoresis in a 3130 Genetic Sequencer.

2.7.1. PCR Reactions Preparation

Reagents from the Amplidex PCR/CE *HTT* kit, we pipetted a mixture containing 5 µL of the HTT PCR Mix and 3 µL of the HTT F;R primer mix. Then 2 µL of DNA (20 ng/ µL) was added into the respective tubes for the final volume of 10 µL. All PCR reactions performed included a negative control and were placed in the Biometra thermal cycler. The table 11 shows the conditions of amplifications.

Table 11- Conditions of the amplifications

Temperature(°C)	Time	Cycles
95	5 min	1 x
97	35 sec	10 X
64	35 sec	
68	4 min	
97	35 sec	18X
64	35 sec	
68	4 min+ 20 sec/cycle	
72	10 min	1 x
4	∞	

2.7.2. Preparation of the samples for capillary electrophoresis

The preparation of the PCR samples for capillary electrophoresis were according to section 2.5.3. However, we pipetted 11 uL of Formamide, 2 uL of ROX1000 and 2 uL of PCR product.

2.7.3. Analysis and Interpretation of Results

Data analysis and interpretation was conducted using the fragment analysis software Gene Mapper (Thermo Fisher Scientific,USA) version 3.7. The electropherograms were analyzed by two independent operators, to quantify the number of repeats CAG, we used 2 methods: i) manually with the identification of the initial peak at~83 bp, corresponding to 5 CAGs and ii) through the proposed correction factors for 3130 Genetic Analyzer (Co=70,4290 and mo=2,8588) provided by protocol.

2.8. Detection of the CAG trinucleotide repeat expansion of the *ATXN3* gene

The detection of CAG trinucleotide repeat expansions in the *ATXN3* gene was performed by the STR- PCR amplification for all the samples, homozygous samples were studied by RP-PCR amplification to confirmation it there was any expanded all not detected by STR-PCR.

2.8.1. STR- PCR Reactions Preparation

The preparation of the amplification reactions of exon 10 was performed by STR-PCR, in which the primers were previously designed in the laboratory. The table 12 shows the sequence of the primers. The mixture of reagents for amplifying the CAG repeat region of the *ATXN*$_3$ gene was prepared to a final volume, 25 uL, according to the table 13. Then 1 µL of DNA (100-150 ng/ µL) was added into the respective tubes. All PCR reactions performed had included a negative control and positive control, and were placed in the Biometra thermal cycle. The amplification conditions are shown in the table 14.

Table 12- Primer Sequence of the *ATXN3* gene

Name	**Sequence (5´-3')**
SCA$_3$ F	CACTTTTGAATGTTTCAGACAGCAG
Fam SCA$_3$ R	TGGCCTTTCACATGGATGTG

Table 13- Reagent used in the STR- PCR mixture to amplify *ATXN3* gene

Reagent	**Final Concentration**	**Volume (uL)**
H_20	-	14.4
Buffer 5x	1 x	5
dNTPs 5mM	0.2 mM	1
$MgCl_2$ 25 mM (Promega)	1.5 mM	1.5
SCA$_3$ F 10 mM	0.5 mM	1
SCA$_3$ R 10 mM	0.5 mM	1
Taq Promega (uL/5U)	0.5U	0.1

Table 14- The amplification conditions of STR-PCR

Steps	Temperature (°C)	Time	Cycles
Initial Denaturation	96	2 min	1 x
Denaturation	96	45 sec	35X
Primers	60	45 sec	
DNA extension	72	1 min	
Final Extension	72	10 min	1X
Cooling	4	∞	

2.8.2. Electrophoresis in Agarose Gel

Confirmation of the amplification products was done by an agarose gel electrophoresis run. This was prepared according to the procedure described in section 2.4.2.

2.8.3. Preparation of the samples for capillary electrophoresis

The preparation of the STR-PCR samples for capillary electrophoresis was according to section 2.5.3. However, we pipetted 9.8 uL of Formamide, 2 uL of LIZ 500 and 2 uL of STR-PCR product.

2.8.4. Analysis and Interpretation of Results

The analysis and interpretation of the results were performed according to the section 2.5.4. However, we used 2 control samples, with known 4 alleles (20, 23, 70 and 71 CAG repeats) to establish linear calibration.

2.8.5. RP- PCR Reactions Preparation

For the preparation of the RP-PCR amplification reactions, primers were previously designed in the laboratory. The table 15 shows the sequence of the primers. The mixture of reagents for amplifying the *ATXN3* gene was performed by RP-PCR reaction to a final volume according to the table 16.

Table 15- Primer Sequence of the exon 10 of the *ATXN3* gene

Name	Sequence (5´-3')
Fam SCA_3 F2	TGTCTAGATTTCCTAAGATCAG

P3	TACGCATCCCAGTTTGAGACG
TP1	TACGCATCCCAGTTTGAGACGCTGCTGCTGCTGCTG

Table 16- Reagents used in the RP- PCR mixture

Reagent	Final Concentration	Volume (uL)
H_20	-	10,75
Buffer 5x	1x	2,5
dNTPs	5 mM	2
GC-RICH solution	5	5
Fam-SCA3 F210mM	0,5uM	1,3
P3, 10µM	0,5uM	1,3
TP1, 10µM	0,5uM	0,65
Pwo SuperYield DNA Polymerase 5U/µl	0,5U	0,5

Then 1 µL of DNA (100-150 ng/ µL) was added into the respective tubes for the final volume of 25 µL. All RP-PCR reactions performed had included a negative control, and were placed in the Biometra thermal cycler. The amplification conditions are shown in the table 17.

Table17- The amplification conditions of RP-PCR

Steps	Temperature (°C)	Time (min)	Cycles
Initial Denaturation	95	5	1 x
Denaturation	95	1	35 x
Primers	50	1	
DNA extension	72	3	
Final Extension	72	10	1 x
Colling	4	∞	

2.8.6. Preparation of the samples for capillary electrophoresis

Preparation of the TP-PCR samples was performed according to the section 2.8.4. However, we pipetted 4 uL of the RP-PCR product.

2.8.7. Analysis and Interpretation of Results

The analysis of results was performed according to the section 2.5.8.

3.1. Analysis of Friedreich Ataxia patients

3.1.1. Study population

In this chapter, we studied 10 patients, with suspected clinical diagnosis of Friedreich's Ataxia. Of those, 5 were males and 5 were females, with the mean age of 53.8 years, who were followed in the neurogenetics consultation.

3.1.2. Mutation analysis of *FXN* gene

In the genetic analysis of the *FXN* gene, no mutations were found in the patients studied.

3.1.3. Implementation of the repeat expansion detection technique in the *FXN* gene

To detect the repeat expansion in the *FXN* gene the kit of Adellgene Friedreich's Ataxia kit was used according to the manufacture instructions. During the implementation of the kit, it was used three control samples to optimize the technique: one control with 1 normal allele and 1 expanded allele, one normal heterozygous control (9 and 22 GAA repeats) and finally one control with 2 expansion alleles (200 and 900 GAA repeats). In Table 18, it can be found the number of GAA repeat expansions alleles of these three controls.

3.1.4. Detection of the GAA repeat expansion in the *FXN* gene

To quantify the number of GAA repeat expansions alleles, we use the values given in the protocol concerning the correlation between the size fragments and number of GAA repeats, as it was already mentioned in section 2.5.4. Not just that, it was also considered the cut-off for Friedreich's Ataxia, as it is shown in Table 19. In Table 18, are presented the number of GAA repeats expansions alleles of the 10 patients studied. As we can see, in none of the patients were found expanded alleles typical of Friedreich's Ataxia.

Table 18- Results of the Analysis of GAA repeat expansion alleles in the *FXN* gene

		Peak Size (bp)	STR-Results	TP-PCR Results	Genotype/Zygosity
Samples used to implement the technique	Control 1	313	9	Expansion	Heterozygous with expansions (9, exp)
	Control 2	313	9	—	Normal
		352	22		Heterozygous (9,22)
	Control 3	—	—	Expansion	Heterozygous with expansions (200,900)
Patients studied	1	308	7	No expansion	Normal Homozygous (7,7)
	2	308	7	No expansion	Normal Homozygous (7,7)
	3	307	7	—	Normal
		313	9		Heterozygous (7,9)
	4	313	9	No expansion	Normal Homozygous (9,9)
	5	307	7	No expansion	Normal Homozygous (7,7)
	6	313	9	No expansion	Normal Homozygous (9,9)
	7	308	7	—	Normal
		352	22		Heterozygous (7,22)
	8	313	9	No expansion	Normal Homozygous (9,9)
	9	307	7	—	Normal
		313	9		Heterozygous (7,9)
	10	_	_	No expansion	Normal Homozygous

Table 19- Mutation category on GAA repeat length in the *FXN* gene

Category	GAA repeat	References
Normal	5-30	(Corben *et al.*, 2014)
Intermediate	30-~49	
Expansion	~50-~1300	

The Figure 5 illustrate the results of the fragment analysis graphs obtained by STR-PCR. (A) results for normal heterozygous individuals. (Patients #3, #7 and #9); (B) results for homozygous individuals (Patients #1, #2, #4, #5, #6; #8 and #10).

Figure 5- Fragment analysis STR-PCR graphs

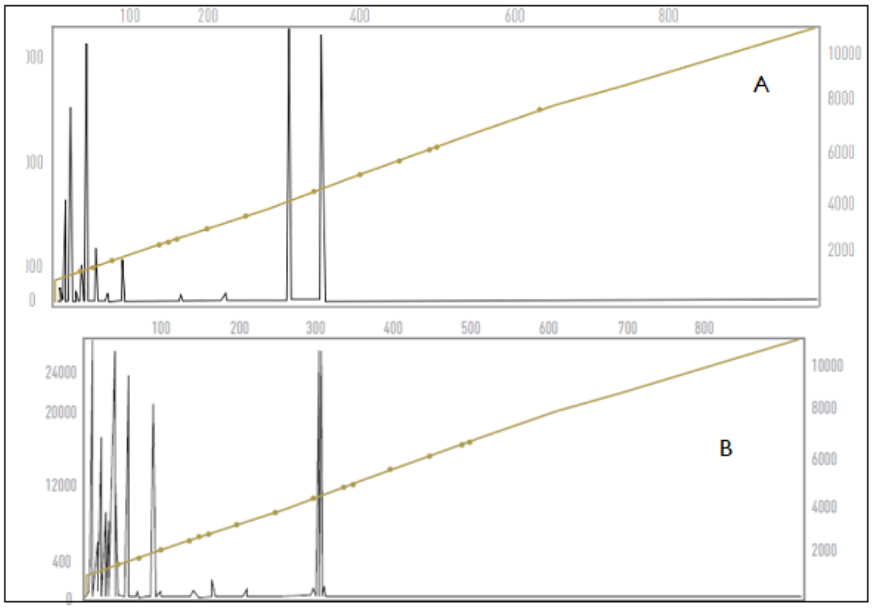

The figure 6 illustrates the results of the fragment analysis graph obtained by TP-PCR with an expanded allele.

Figure 6- Fragment analysis TP-PCR graph

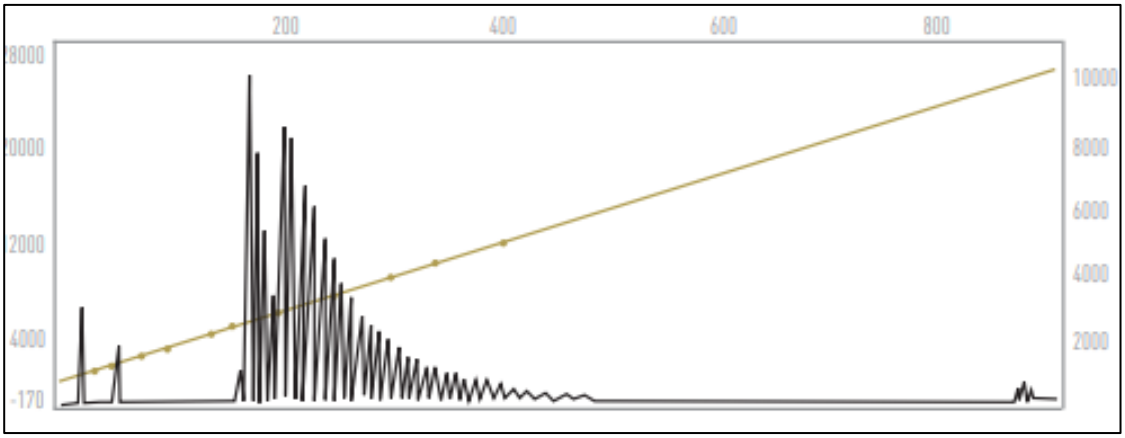

3.2. Analysis of the G_4C_2 repeat expansion in the *C9orf72* gene

3.2.1. Study population

In this chapter, we studied 56 individuals (25 were males and 31 were females, with the mean age of 56.31 years). Of those, 42 were patients followed in the Dementia

consultation and 14 were family relatives still asymptomatic. All the patients were previously studied, between 2012-2022 and their mutation analysis revealed that all of them carried the pathogenic expansion of G_4C_2. The detection of this expansion was performed using an in-house technique, developed in the Neurogenetics laboratory according to (Zee, van der *et al.*, 2013). However, using this technique, it was not able to size the number of hexanucleotide repeats expansions. For that reason, we set up a new method to quantify the number of repeat expansions, using Asuragen Amplidex® PCR/CE *C9orf72* kit. The patients included: 25 FTLD cases, 13 ALS cases and 4 FTLD-ALS cases, as illustrated in the Figure 7.

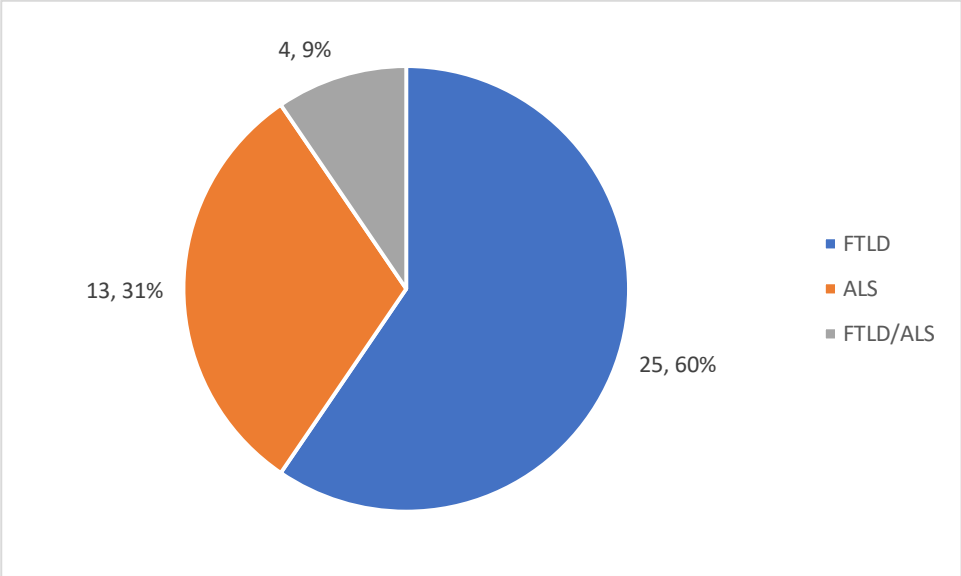

Figure 7- Percentage of FTLD, ALS and FTD-ALS patients

3.2.2. Implementation of the repeat expansion detection technique in the *C9orf72* gene

To detect the hexanucleotide repeat expansion in the *C9orf72* the kit of Asuragen Amplidex® PCR/CE *C9orf72* kit was used according to the manufacture instructions. During the implementation of the kit, it was used four control samples to optimize the technique: one normal homozygous control (2 G_4C_2 repeats), one normal heterozygous control (2 and 12 G_4C_2 repeats), two heterozygous controls, with an expanded allele (2,>145 and 10,>145 G_4C_2 repeats). In Table 20, are represented the number of G_4C_2 repeat expansion allele of these four controls.

3.2.3. Detection of the G_4C_2 repeat expansion in the *C9orf72* gene

To quantify the number of repeats G_4C_2 we used 3 different methods: 1) the AmplideX_PCR_CE, where the software gives us the number of G_4C_2 repeat expansion automatically, 2) through the proposed correction factors for 3500 Genetic Analyzer

(Co=117.7 and mo=5.8), and 3) according to the established linear calibration curve generated by the 4 peaks of known repeat lengths of the PCR control sample provided by the kit., as it was already mentioned in section 2.6.3. The cut-off values considered can be found in Table 21. The number of G_4C_2 repeat expansion allele of the patients are shown in Table 20.

Table 20- Results of the Analysis of the G_4C_2 repeat expansion in the *C_9orf_{72}* gene

		Peak size (bp)	**1)**	**2)**	**3)**
Samples used to implement the technique	Control 1	128	2	1.8	1.9
	Control 2	128	2	1.8	1.9
		190	12	12.5	11.6
	Control 3	127	2,>145	1.6	1.7
	Control 4	179	10,>145	10.6	9.9
Patients studied	29	126	2,>145	1.4	1.8
		127		1.6	2.0
		126		1.4	1.7
		127		1.6	1.9
		126		1.4	1.7
		127		1.6	1.9
		128		1.8	1.9
		128		1.8	1.8
	1	127	2,63	1.6	1.9
		591		65.6	59.4
	1	126	2,78	1.4	1.8
		498		81.6	73.9
	1	142	3,>145	4.2	4.2
	4	148	4,>145	5.2	5.2
		147		5.1	5.0
	2	154	6,>145	6.3	6.0
	6	166	7,>145	8.3	8.0
		160		7.3	6.9
	1	165	7,38	8.2	7,9
		350		40.1	36.5
	3	166	8,>145	8.3	8.0
				8.3	7.9
	2	178	9,>145	10.2	9.7
				10.4	9.8
	3	179	10,>145	10.6	9.9
		184		11.4	10.7
	3	189	11,>145	12.3	11.6
		190		12.5	11.8

Table 21- Mutation category based G_4C_2 repeat length in the *C9orf72* gene

Category	G_4C_2 Repeat	References
Normal	<20	(Majounie *et al.*, 2012)
Intermediate	20-30	
Expansion	>30 and often >1000	

The Figure 8 illustrate the results of the fragment analysis graphs. (A) results for normal heterozygous individuals (Control 2); (B) results for heterozygous individuals with an expanded allele. (All Patients)

Figure 8- Fragment analysis graphs

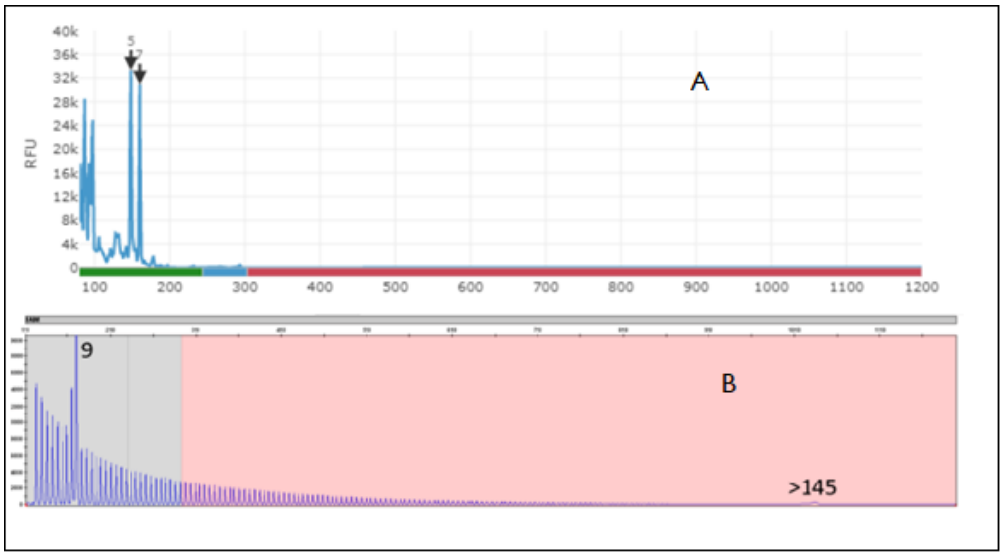

3.3. Analysis of the CAG repeat expansion in the *HTT* gene

3.3.1. Study population

In this chapter, we studied 10 patients, with suspected clinical diagnosis of Huntington's Disease. Of those, 4 were males and 6 were females, with a mean age of 70.22 years, who were followed in the neurogenetics consultation. Out of the 10 patients, 5 carried the pathogenic expansion CAG, typical of Huntington's Disease.

3.3.2. Implementation of the repeat expansion detection technique in the *HTT* gene

To detect the repeat expansion in the *HTT* gene Asuragen Amplidex®PCR/CE *HTT* kit was used according to the manufacture instructions. During the implementation of the kit, it

was used three control samples: two heterozygous controls with an expanded allele (17, 40 and 17, 45 GAA repeats), one normal heterozygous control heterozygous (10 and 15 CAG repeats). In Table 22, are represented the number of CAG repeat expansions alleles of these three controls.

3.3.3. Detection of the CAG repeat expansion in the *HTT* gene

To quantify the number of repeats CAG, were used 2 methods: 1) manually with the identification of the initial peak at~83 bp, corresponding to 5 CAGs and 2) through the proposed correction factors for 3130 Genetic Analyzer (Co=70.4290 and mo=2.8588) provided by the protocol, as it was already mentioned in the section 2.7.3. It was also considered the cut off values found in Table 23. Table 22 shows the number of CAG repeat expansion allele of these patients.

Table 22- Results of the analysis of the CAG repeat expansion in the *HTT* gene

		Peak Size (bp)	**1)**	**2)**	**Genotype/Zygosity**
Samples used to implement the technique	Control 1	119	17	17	Heterozygous with expansions (17,45)
		199	45	45	
	Control 2	119	17	17	Heterozygous with expansions (17,40)
		185	40	40	
	Control 3	98	10	10	Normal Heterozygous (10,15)
		113	15	15	
Patients studied	1	122	18	18	Heterozygous with expansions (18,40)
		185	40	40	
	2	122	18	18	Normal Heterozygous (18,19)
		125	19	19	
	3	119	17	17	Heterozygous with expansions (17,41)
		188	41	41	
	4	137	23	23	Heterozygous with expansions (23,42)
		191	42	42	
	5	97	10	9	Heterozygous with expansions (10,41)
		185	41	40	
	6	120	18	17	Normal Homozygous (18,18)
	7	120	18	17	Normal Homozygous (18,18)
	8	118	17	17	Normal Heterozygous (17,18)
		121	18	18	
	9	127	20	20	Heterozygous with expansions (20,43)
		192	43	42	
	10	118	17	17	Normal Heterozygous (17,18)
		121	18	18	

Table 23- Mutation category based on CAG repeat length in the *HTT* gene

Category	CAG Repeat	References
Normal	≤26	(Bean e Bayrak-Toydemir, 2014)
Intermediate	27-35	
Reduced Penetrance	36-39	
Expansion	≥40	

The Figure 9 illustrate the results of the fragment analysis graphs. (A) results for normal heterozygous individuals (Patients #2, #8 and #10); (B) results for heterozygous individuals with an expanded allele (Patients #1, #3, #4, #5 and #9).

Figure 9- Fragment analysis graphs

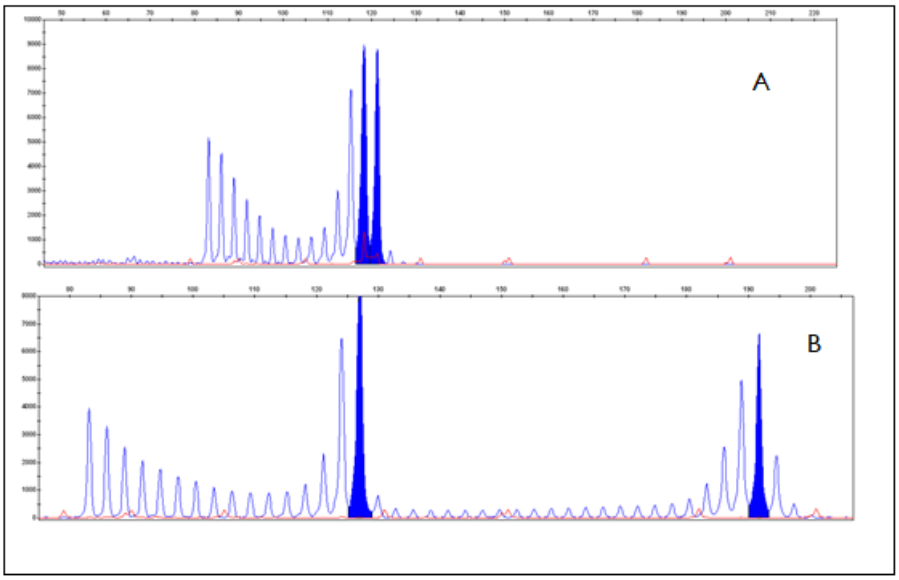

3.4. Analysis of the CAG repeat expansion in the *ATXN3* gene

3.4.1. Study population

In this chapter, we studied 16 patients with suspected clinical diagnosis of Machado Joseph Disease. Of those, 10 were males and 6 were females, with a mean age 49.53 years, who were followed in the neurogenetics consultation. Out of the 16 patients, 4 carried the pathogenic expansion CAG, typical of Machado Joseph Disease.

3.4.2. Implementation of the repeat expansion detections technique in the *ATXN3* gene

To implement and optimize the in-house technique, five samples were used: two three heterozygous with an expanded allele (18, 71, 20, 70, 23, 71 CAG repeats) and normal heterozygous controls (14, 23 and 36 CAG repeats). The number CAG repeat expansion allele were presented in Table 24.

3.4.3. Detection of the CAG repeat expansion in the *ATXN3* gene

To quantify the number of repeats CAG, we used 2 control samples, with known 4 alleles (20, 23, 70 and 71 CAG repeats) to establish linear calibration, as it was already mentioned in section 2.8.4. It was considered the cut-off values, which is shown in Table 25. In Table 24, it can be found the analysis of the number of CAG repeat expansion allele of these patients.

Table 24- Results of the Analysis of the CAG repeat expansion in the *ATXN3* gene

		Peak size (bp)	STR-PCR Results	TP-PCR Results	Genotype/Zygosity
Samples used to implement the technique	Control 1	119	20	expansions	Heterozygous with expansions (20, 70)
		260	70		
	Control 2	128	23	expansions	Heterozygous with expansions (23,71)
		262	71		
	Control 3	128	23	no expansions	Normal Heterozygous (23,36)
		168	36		
	Control 4	113	18	expansions	Heterozygous with expansions (18,71)
		263	71		
	Control 5	102	14	no expansions	Normal Heterozygous (14,23)
		128	23		
Patients studied	1	128	23	expansions	Heterozygous with expansions (23,65)
		246	65		
	2	101	14	expansions	Heterozygous with expansions (14,69)
		259	69		
	3	101	14	expansions	Heterozygous with expansions (14,75)
		274	75		
	4	101	14	no expansions	Normal Heterozygous (14,27)
		139	27		
	5	127	23	no expansions	Normal Heterozygous (23,27)
		139	27		
	6	113	18	no expansions	Normal Heterozygous (18,23)
		127	23		
	7	102	14	no expansions	Normal Heterozygous (14,28)
		142	28		

	8	130	24	no expansions	Normal Heterozygous (24,30)
		149	30		
	9	102	14	no expansions	Normal Heterozygous (14,23)
		128	23		
	10	102	14	no expansions	Normal Heterozygous (14,28)
		141	28		
	11	102	14	no expansions	Normal Heterozygous (14,25)
		135	25		
	12	128	23	no expansions	Normal Heterozygous (23,27)
		140	27		
	13	140	27	no expansions	Normal Heterozygous (27,31)
		150	31		
	14	103	14	no expansions	Normal Homozygous (14,14)
	15	127	23	expansions	Heterozygous with expansions (23,72)
		266	72		
	16	128	23	no expansions	Normal Heterozygous (23,24)
		131	24		

Table 25- Mutation category based on CAG repeat length in the *ATXN3* gene

Category	CAG repeats	References
Normal	11-44	(Sequeiros, Martindale e Seneca, 2010)
Intermediate	45-52	
Expansion	53	

The Figure 10 illustrate the results of the fragment analysis graphs obtained by STR-PCR. (A) results for normal heterozygous individuals (Patients #4, #5, #6, #7, #8, #9, #10, #11, # 12, #13 and #16); (B) results for heterozygous individuals with an expanded allele (Patients #1, #2, #3, and #15).

Figure 10- Fragment analysis STR-PCR graphs

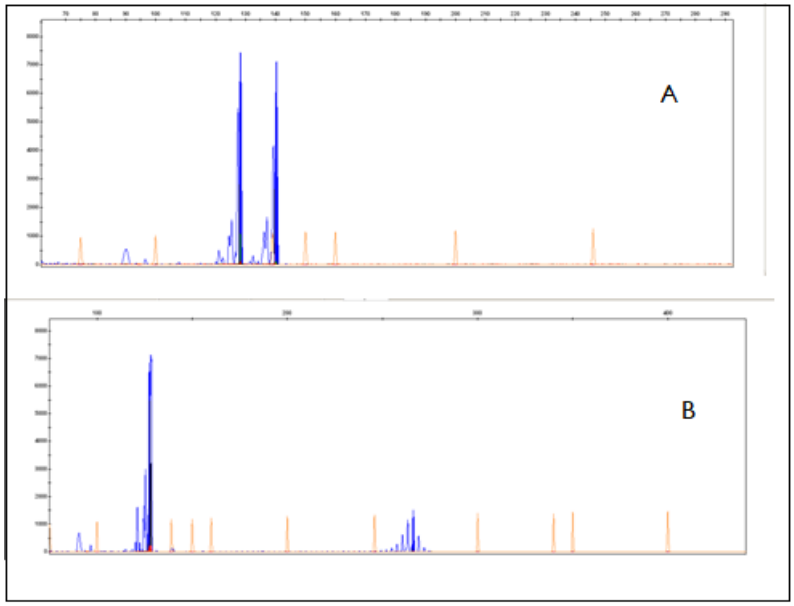

The figure 11 illustrates the results of the fragment analysis graph obtained by RP-PCR with an expanded allele.

Figure 11- Fragment analysis RP-PCR graph

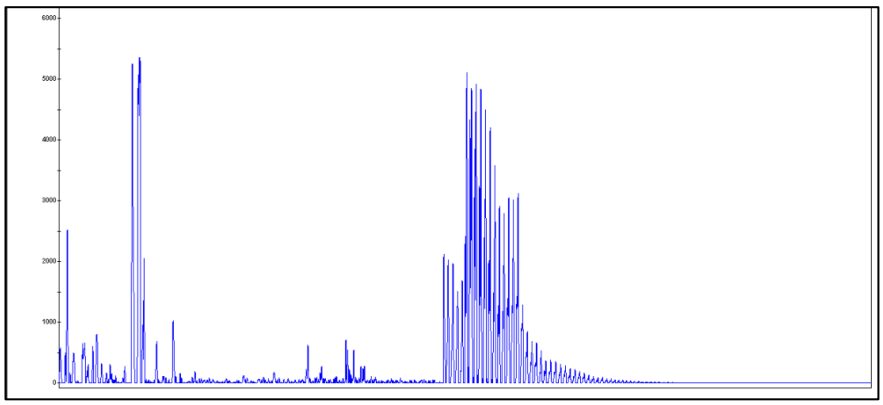

4. Discussion

In the present study we have genetic characterized patients with repeat expansion disorders, such as: Friedreich's Ataxia, Frontotemporal Lobar Degeneration, Amyotrophic Lateral Sclerosis, Huntington's disease and Machado Joseph disease.

We started with the study of 10 patients, with suspected clinical diagnosis of Friedreich's Ataxia and we didn't find any mutations in the *FXN* gene on any of the patients. Indeed, in literature a few mutations have been reporter in this gene accounting only for 5% of the cases. These mutations included W168R, described by (Clark *et al.*, 2019), found in exon 5. One mutation G130V, described by (Delatycki *et al.*, 1999), located in exon 4 and R165C, described by (Clark *et al.*, 2017), identified in homozygous patients in exon 5. Also, W155R, W155A, W155F and I154F, described by (Tsai, Bridwell-Rabb e Barondeau, 2011), in exon 4.

Interestingly in our cohort of patients, none of the patients had the pathogenic GAA repeat expansions in *FXN* gene, typical of the Friedreich's Ataxia, according to the established cut-off values. Therefore, it was not possible to correlate the clinical symptoms of the patients with the size of the GAA repeat expansion. This would be important as it has not yet been described in the literature.

Most of our patients are normal homozygous, (7 patients), while the remaining, 3 patients are heterozygous with the allele sizes ranging from 9 to 22 repeats.

The second repeat expansions diseases studied were FTLD and/or ALS. Thus, we studied 25 FTLD patients, 13 ALS and 4 have both forms of the diseases. All these patients were selected based on their genetic status, since all of them carried the pathogenic G_4C_2 expansion in the C_9orf_{72} gene. According to (Rohrer *et al.*, 2015) and (Majounie *et al.*, 2012), the most common form of FTLD associated to the mutation of gene C_9orf_{72} is bvFTD. Curiously, all of the 25 patients diagnosed with FTLD had this variant associated, which in the line with previously reported.

With the quantification of the number of G_4C_2 repeat expansions on C_9orf_{72} gene, with the different methods already mentioned in section 3.2.3, we can see that, the best method to calculate the number of G_4C_2 repeat expansions is a linear calibration curve generated by 4 peaks with known length of the PCR control sample provided by the kit, in which the size of the peaks is converted in repeat size, according to the equation described in section 2.5.4. Comparing this method to the ones previously reported, this one showed the best results.

In most of our patients, the number of G_4C_2 repeat expansion in *C_9orf_{72}* gene, was higher than 145 repeats. Hence, it was not possible to quantify the size of long expansions, due to the upper limit of the repeat- primed detection method, which was Asuragen Amplidex® PCR/CE *C_9orf_{72}* kit. However, there were 3 patients with smaller expanded alleles such as: 38, 63 and 78 repeats. It is important to mention, that there was no clear consensus on which *C_9orf_{72}* repeat length is pathogenic, which poses a major challenge for clinical genetic counselling.

We can also see that our patients were heterozygous to the G_4C_2 repeat expansion with most common allele found had 2 repeats.

The third expansions disease studied was Huntington's Disease. Our cohort of patients included 10 suspected individuals, 3 of which were normal heterozygous with the size alleles within the normal range (<23 repeats), whereas 5 patients carried the pathogenic CAG expansion (>40 repeats). It is important to mention, that Huntington's Disease was associated with the phenomenon of anticipation, therefore the genetic counseling of these affected individuals is crucial. There were also 2 normal homozygous patients. The method used to quantify the number of CAG expansion repeats, which was the best method to use, was manual counting, with the identification of the initial peak at~83 bp, corresponding to 5 CAGs.

In compliance with (Podvin *et al.*, 2019), our patients cohort diagnosed with Huntington's disease had number of CAG repeat expansions between 40 and 53 repeats.

In contrast with (Cui *et al.*, 2017), none of the patients have tics as first symptoms. Indeed, most of our patients have as first clinical manifestation, involuntary movements, also known as chorea and there were also some of the patients with imbalance and difficulty moving.

The last repeat expansions diseases studied was Machado Joseph disease. Out of the 16 patients studied, 12 were normal (11 heterozygous and 1 homozygous), with the size off alleles ranging from 14 to 27 repeats. It is important to mention, that Machado Joseph Disease was associated with the phenomenon of anticipation, therefore the genetic counseling of these affected individuals is crucial to predict the outcome of future generation.

We tried to correlate the 5 types of the disease with our patients, but wasn't possible because all of them have the same type. Interestingly, all of our Machado Joseph patients belong to type II of the disease which is in line with previously reported (Lin *et al.*, 2018).

In contrast with (Lin *et al.*, 2018), none of the patients have spastic paraparesis as first symptoms. Indeed, most of our patients have imbalance while walking as their first symptom. Again, it was not possible to establish correlations due to the small size of our cohort.

Finally, in this study, we were able to quantify the repeat expansions alleles present in 65 individuals, including: 56 with Frontotemporal Lobar Degeneration and/or Amyotrophic Lateral Sclerosis, 5 with Huntington's disease and 4 with Machado Joseph disease.

5.Conclusion and Future Perspective

In this study, we set up several molecular approaches to detect the pathological expansions in patients with different repeat expansions disorders such as: Friedreich's Ataxia, Frontotemporal Lobar Degeneration, Amyotrophic Lateral Sclerosis, Huntington's Disease and Machado Joseph Disease using commercial kits and/or *in*-house methods.

Thus, using different methods, we were able to quantify the number of DNA repeats in the different patients recruited, providing a molecular diagnosis.

The molecular diagnosis of Friedreich's Ataxia included the detection of point mutations in the *FXN* gene and the detection of the number of GAA repeat expansions in this gene. Therefore, in the present study, we started optimizing the mutations analysis in the *FXN* gene using Sanger sequencing with subsequently analysis of the GAA repeat expansions using the Adellgene Friedreich's Ataxia kit. In none of the patients studied were identified any point mutations or pathogenic repeat expansions. Thereby, we could not confirm the Friedreich's Ataxia diagnosis in any of the patients referred with the suspected clinical diagnosis of Friedreich's Ataxia.

The molecular diagnosis of Frontotemporal Lobar Degeneration and Amyotrophic Lateral Sclerosis is done by detecting the number of G_4C_2 repeat expansion repeats in the C_9orf_{72} gene, and/or by the identification of pathogenic mutations in one of the genes associated with these diseases. For this study, only the detection of the number of repeats in C_9orf_{72} was assessed.

For these two diseases, all of the recruited patients carried the pathogenic G_4C_2 expansion, previously identified by an in-house method in the laboratory of Neurogenetics, although the size of the repeat expansion allele was not determined thus far. Therefore, in the present study, a new method was set up to quantify the size of the expanded allele using the Asuragen Amplidex PCR/CE C_9orf_{72} kit. Thus, in our study 53 individuals were identified with one expanded allele with more than 145 G_4C_2 repeats, while 3 patients harbor a smaller expanded allele ranging from 38-78 repeats. In the future this method will be included in the laboratory in a routine basis to evaluate these patients.

In addition, the molecular diagnosis of Huntington's disease was done by detecting the number of CAG repeat expansions in the *HTT* gene using the Asuragen Amplidex PCR/CE *HTT* kit method. In the present study, we were able to confirm the molecular diagnosis of five patients who harbor an expanded allele ranging from 40 to 43 CAG repeats. Due to the small

size off our cohort of patients, we could not correlate the expansion size to the patient's clinical manifestations. More data is needed, to do such correlations.

The molecular diagnosis of Machado Joseph disease was done by detecting the number of CAG repeats expansions in the *ATXN3* gene, with an in house STR-PCR and RP-PCR method. Again, we could not correlate the expansion size to the clinical manifestations of the patients or to the five subtypes of Machado Joseph Disease, since only 4 patients were identified as having an expanded allele typical of Machado Joseph Disease. More data is needed, to establish genotype-phenotype correlations.

So in terms of future perspectives, we aim to increase the number of patients studied with these different repeat expansions disorders in order to be able to establish genotype-phenotype particularly correlations between the expansion size and the clinical manifestations of the patients.

6.References

BANG, Jee; SPINA, Salvatore; MILLER, Bruce L. - Frontotemporal dementia. **The Lancet**. . ISSN 1474547X. 386:10004 (2015) 1672–1682. doi: 10.1016/S0140-6736(15)00461-4.

BEAN, Lora; BAYRAK-TOYDEMIR, Pinar - American college of medical genetics and genomics standards and guidelines for clinical genetics laboratories, 2014 edition: Technical standards and guidelines for huntington disease. **Genetics in Medicine**. . ISSN 15300366. 16:12 (2014) e2. doi: 10.1038/gim.2014.146.

BETTENCOURT, Conceição; LIMA, Manuela - Machado-Joseph disease: From first descriptions to new perspectives. **Orphanet Journal of Rare Diseases**. . ISSN 17501172. 6:1 (2011) 1–12. doi: 10.1186/1750-1172-6-35.

CASTALDO, I. *et al.* - DNA methylation in intron 1 of the frataxin gene is related to GAA repeat length and age of onset in Friedreich ataxia patients. **Journal of Medical Genetics**. . ISSN 00222593. 45:12 (2008) 808–812. doi: 10.1136/jmg.2008.058594.

CASTRO, Ignacio Hugo *et al.* - Frataxin Structure and Function. Em **Subcellular Biochemistry** [Em linha]. Springer, Cham, 2019 [Consult. 28 mai. 2022]. Disponível em WWW:<URL:https://link.springer.com/chapter/10.1007/978-3-030-28151-9_13>.v. 93. p. 393–438.

CLARK, Elisia *et al.* - Selected missense mutations impair frataxin processing in Friedreich ataxia. **Annals of Clinical and Translational Neurology**. . ISSN 23289503. 4:8 (2017) 575–584. doi: 10.1002/acn3.433.

CLARK, Elisia *et al.* - Identification of a novel missense mutation in Friedreich's ataxia – FXNW168R. **Annals of Clinical and Translational Neurology**. . ISSN 23289503. 6:4 (2019) 812–816. doi: 10.1002/acn3.728.

COOK, A.; GIUNTI, P. - Friedreich's ataxia: Clinical features, pathogenesis and management. **British Medical Bulletin**. . ISSN 14718391. 124:1 (2017) 19–30. doi: 10.1093/bmb/ldx034.

CORBEN, Louise A. *et al.* - Consensus clinical management guidelines for Friedreich ataxia. **Orphanet Journal of Rare Diseases**. . ISSN 17501172. 9:1 (2014). doi: 10.1186/s13023-014-0184-7.

CUI, Shi Shuang *et al.* - Tics as an initial manifestation of juvenile Huntington's disease: Case report and literature review. **BMC Neurology**. . ISSN 14712377. 17:1 (2017). doi:

10.1186/s12883-017-0923-1.

DELATYCKI, M. B. *et al.* - Sperm DNA analysis in a Friedreich ataxia premutation carrier suggests both meiotic and mitotic expansion in the FRDA gene. **Journal of Medical Genetics**. . ISSN 00222593. 35:9 (1998) 713–716. doi: 10.1136/jmg.35.9.713.

DELATYCKI, Martin B. *et al.* - G130V, a common FRDA point mutation, appears to have arisen from a common founder. **Human Genetics**. . ISSN 03406717. 105:4 (1999) 343–346. doi: 10.1007/s004399900142.

DELATYCKI, Martin B.; BIDICHANDANI, Sanjay I. - Friedreich ataxia- pathogenesis and implications for therapies. **Neurobiology of Disease**. . ISSN 1095953X. 132:2019). doi: 10.1016/j.nbd.2019.104606.

DEPIENNE, Christel; MANDEL, Jean Louis - 30 years of repeat expansion disorders: What have we learned and what are the remaining challenges? **American Journal of Human Genetics**. . ISSN 15376605. 108:5 (2021) 764–785. doi: 10.1016/j.ajhg.2021.03.011.

ELLERBY, Lisa M. - Repeat Expansion Disorders: Mechanisms and Therapeutics. **Neurotherapeutics**. . ISSN 18787479. 16:4 (2019) 924–927. doi: 10.1007/s13311-019-00823-3.

INDELICATO, Elisabetta *et al.* - Onset features and time to diagnosis in Friedreich's Ataxia. **Orphanet Journal of Rare Diseases**. . ISSN 17501172. 15:1 (2020). doi: 10.1186/s13023-020-01475-9.

JANUARIO, Cristina (2011)- ***Doença de Huntington Onde estamos agora?***

LIN, Hui Chen *et al.* - Spastic paraparesis as the first manifestation of Machado-Joseph disease: A case report and review of the literature. **Clinical Neurology and Neurosurgery**. . ISSN 18726968. 172:May (2018) 137–140. doi: 10.1016/j.clineuro.2018.06.037.

LUCA, Alessandro DE *et al.* - A novel triplet-primed pcr assay to detect the full range of trinucleotide cag repeats in the huntingtin gene (Htt). **International Journal of Molecular Sciences**. . ISSN 14220067. 22:4 (2021) 1–13. doi: 10.3390/ijms22041689.

MAJOUNIE, Elisa *et al.* - Frequency of the C9orf72 hexanucleotide repeat expansion in patients with amyotrophic lateral sclerosis and frontotemporal dementia: A cross-sectional study. **The Lancet Neurology**. . ISSN 14744465. 11:4 (2012) 323–330. doi: 10.1016/S1474-4422(12)70043-1.

MASRORI, P.; DAMME, P. VAN - Amyotrophic lateral sclerosis: a clinical review. **European**

Journal of Neurology. . ISSN 14681331. 27:10 (2020) 1918–1929. doi: 10.1111/ene.14393.

MCCOLGAN, P.; TABRIZI, S. J. - Huntington's disease: a clinical review. **European Journal of Neurology**. . ISSN 14681331. 25:1 (2018) 24–34. doi: 10.1111/ene.13413.

NOPOULOS, Peggy C. - Huntington disease: A single-gene degenerative disorder of the striatum. **Dialogues in Clinical Neuroscience**. . ISSN 12948322. 18:1 (2016) 91–98. doi: 10.31887/dcns.2016.18.1/pnopoulos.

OLNEY, Nicholas T.; SPINA, Salvatore; MILLER, Bruce L. - Frontotemporal Dementia. **Neurologic Clinics**. . ISSN 15579875. 35:2 (2017) 339–374. doi: 10.1016/j.ncl.2017.01.008.

ORPHANET - **Orphanet: About rare diseases** [Em linha], atual. 2016. [Consult. 13 jul. 2022]. Disponível em WWW:<URL:https://www.orpha.net/consor/cgi-bin/Education_AboutRareDiseases.php?lng=EN>.

PAULSON, Henry - Repeat expansion diseases. Em **Handbook of Clinical Neurology**. ISBN 9780444632333v. 147. p. 105–123.

PODVIN, Sonia *et al.* - Multiple clinical features of Huntington's disease correlate with mutant HTT gene CAG repeat lengths and neurodegeneration. **Journal of Neurology**. . ISSN 14321459. 266:3 (2019) 551–564. doi: 10.1007/s00415-018-8940-6.

ROHRER, Jonathan D. *et al.* - C9orf72 expansions in frontotemporal dementia and amyotrophic lateral sclerosis. **The Lancet Neurology**. . ISSN 14744465. 14:3 (2015) 291–301. doi: 10.1016/S1474-4422(14)70233-9.

SEQUEIROS, Jorge; MARTINDALE, Joanne; SENECA, Sara - EMQN Best Practice Guidelines for molecular genetic testing of SCAs. **European Journal of Human Genetics**. . ISSN 10184813. 18:11 (2010) 1173–1176. doi: 10.1038/ejhg.2010.8.

SILVERMAN, Hannah E.; GOLDMAN, Jill S.; HUEY, Edward D. - Links Between the C9orf72 Repeat Expansion and Psychiatric Symptoms. **Current Neurology and Neuroscience Reports**. . ISSN 15346293. 19:12 (2019). doi: 10.1007/s11910-019-1017-9.

SCHWANKER, Albert-. Molecular Biology of the cell. 6ª Ed. WW Norton & Co: 2015. ISBM-9780815344322

SMEYERS, Julie; BANCHI, Elena Gaia; LATOUCHE, Morwena - C9ORF72: What It Is, What It Does, and Why It Matters. **Frontiers in Cellular Neuroscience**. . ISSN 16625102. 15:2021). doi: 10.3389/fncel.2021.661447.

TSAI, Chi Lin; BRIDWELL-RABB, Jennifer; BARONDEAU, David P. - Friedreichs ataxia

variants I154F and W155R diminish frataxin-based activation of the iron-sulfur cluster assembly complex. **Biochemistry**. . ISSN 00062960. 50:29 (2011) 6478–6487. doi: 10.1021/bi200666h.

UEYAMA, Morio; NAGAI, Yoshitaka - Repeat expansion disease models. **Advances in Experimental Medicine and Biology**. . ISSN 22148019. 1076:2018) 63–78. doi: 10.1007/978-981-13-0529-0_5.

ZEE, Julie VAN DER *et al.* - A Pan-European Study of the C9orf72 Repeat Associated with FTLD: Geographic Prevalence, Genomic Instability, and Intermediate Repeats. **Human Mutation**. . ISSN 10597794. 34:2 (2013) 363–373. doi: 10.1002/HUMU.22244.